Reviewed Preprint
v1 • December 19, 2024
Not revised

Reviewed Preprint
v2 • July 23, 2026
Revised by authors

For correspondence:
yangsun@stanford.edu

† These authors contributed equally to this work.

Competing interests: No competing interests declared

Funding: See page 17

Reviewing editor: Xiaorong Liu, University of Virginia, United States



# Defective Neuronal Differentiation in Lowe Syndrome is Associated with Mitochondrial Dysfunction and Impaired Cilia-related Sonic Hedgehog Signaling

**Grzegorz Walkiewicz[1,†], Siyu Chen[1,†], Chien-Hui Lo[1,†], Jingyu Zhao[1], Zhiquan Liu[1], Biao Wang[1], Benjamin Lawson[1], Qing Wang[1], Tia J Kowal[1], Yang Sun[1,2,3,4]**

[1]Department of Ophthalmology, Stanford University School of Medicine, Palo Alto, United States • [2]Palo Alto Veterans Administration, Palo Alto, United States • [3]Maternal Children Health Research Institute at Stanford, Stanford University School of Medicine, Palo Alto, United States • [4]BioX, Stanford University School of Medicine, Palo Alto, United States

## eLife Assessment

This study investigated mitochondrial dysfunction and the impairment of the ciliary Sonic Hedgehog signaling in Lowe syndrome (LS), a timely topic given the limited research in this area. The data obtained from patient-derived iPSC neurons and a mouse model are **solid**. Although the main claims of the study are only partially supported by the current evidence, it provides a **useful** starting point for future functional studies investigating the link between mitochondrial defects and primary cilia in neural development.

https://doi.org/10.7554/eLife.104055.2.sa2

## Abstract

Human brain development requires tight coordination of metabolic and signaling pathways. Lowe syndrome (LS) is a recessive X-linked disorder characterized by proximal tubular renal disease, congenital cataracts, glaucoma, and neurodevelopmental delays. While LS results from mutations in the *OCRL* gene, which encodes an inositol polyphosphate 5-phosphatase, the cellular mechanisms driving neuronal dysfunction remain poorly understood. In this study, using patient-derived iPSC neurons, an *OCRL* knockout mouse model, and an independent zebrafish OCRL-deficient model, we identified mitochondrial dysfunction as a conserved phenotype of OCRL loss across species. Collectively, our findings showed that OCRL deficiency leads to reduced mitochondrial activity, decreased mtDNA levels, reduced mitochondrial content (TOM20), and increased oxidative stress. We further showed that OCRL-deficient neural cells exhibited an altered balance of neuronal versus astrocytic differentiation, rather than a defect in neurogenesis. Additionally, we observed impaired Sonic Hedgehog (Shh) signaling and ciliary homeostasis. Thus, we propose that mitochondrial dysfunction-induced oxidative stress acts as a central mediator linking OCRL loss to altered cell fate and disrupted Shh signaling, providing a unifying framework for these phenotypes.

## 1. Introduction

Lowe syndrome (LS) (OMIM #309000) is a rare X-linked disorder characterized by bilateral congenital cataracts, glaucomatous optic nerve degeneration, renal tubular dysfunction, and intellectual disability. The syndrome results from mutations in the oculocerebrorenal syndrome of Lowe gene (*OCRL*), which encodes an inositol polyphosphate 5-phosphatase that primarily hydrolyzes phosphatidylinositol 4,5-bisphosphate (PI(4,5)P2) to generate PI4P (Lewis et al., 1993;

Luscher et al., 2019; Prosseda et al., 2017; Sakakibara et al., 2022; Sharma et al., 2015). Through its role in phosphoinositide metabolism, *OCRL* regulates key cellular processes including membrane trafficking, cytoskeletal organization, and intracellular signaling. Neurologically, patients with LS often exhibit developmental delays, intellectual disability, absent deep tendon reflexes, and hypotonia (Bökenkamp and Ludwig, 2016; Lewis et al., 1993). Nevertheless, the diagnosis of LS remains complicated due to the heterogeneity of its clinical presentation and overlap with other metabolic and neurodevelopmental disorders. This underscores the need for better-defined molecular mechanisms and potential biomarkers that could aid in diagnosis and disease stratification.

Several case reports point to the existence of a link between mitochondrial dysfunction and the pathogenesis of LS: (1) One report described a 5-year-old boy with *OCRL* mutation-confirmed LS who was initially diagnosed with mitochondriopathy based on electron microscopic evidence of mitochondrial abnormalities (Dumic et al., 2020). (2) Another patient, initially suspected of having chronic progressive external ophthalmoplegia (CPEO) due to mitochondrial disease, was later found to carry a missense mutation in *OCRL* (Craigen et al., 2013). Mitochondrial involvement in LS remains poorly defined, and the mechanisms linking *OCRL* function to mitochondrial homeostasis are not understood.

Increasing evidence demonstrates that reactive oxygen species (ROS) levels and mitochondrial DNA damage levels play an important role in directing neural stem cell (NSC) differentiation toward either neuronal or astroglial lineages (Adusumilli et al., 2021; Shahin et al., 2023; Wang et al., 2011). Previous studies have also established that astrocytes maintain their function independently of mitochondrial DNA integrity, while mitochondrial metabolism significantly contributes to astrocyte activation (Ignatenko et al., 2018; Wang et al., 2011). Astrocytes are essential for maintaining multiple critical functions in the central nervous system (CNS), including ionic balance, blood-brain barrier integrity, synaptic function, and metabolic homeostasis (Cabezas et al., 2014; McNeill et al., 2021; Oksanen et al., 2019; Pociūtė et al., 2024). In response to CNS injury, disease, or infection, astrocytes undergo a diverse array of morphological, molecular, and functional changes that are referred to as reactive astrogliosis (Escartin et al., 2021; Matusova et al., 2023; Zamanian et al., 2012). However, how metabolic stress, particularly mitochondrial dysfunction, modulates astrocyte behavior and neural lineage specification in neurodevelopmental disorders remains unclear. Based on these observations, we investigated the role of OCRL in mitochondrial dysfunction and increased oxidative stress in neuronal and astrocyte differentiation.

# 2. Results

## 2.1. Distinct differentiation of neuronal stem cells and neuronal progenitor cells (NSPCs) in *OCRL* knockout and LS iPSCs

To assess whether OCRL loss-of-function affects neuronal lineage specification, we employed an *in vitro* model of induced neurons (iNs) differentiated from Lowe syndrome (LS) patient-derived induced pluripotent stem cells (iPSCs) using a rapid single-step direct conversion protocol (Zhang et al., 2013). The LS iPSC line (LS100) was derived from a 17-year-old male patient clinically diagnosed with LS following genetic confirmation of an OCRL mutation. In contrast, the familial control line (LS200) originated from his 22-year-old unaffected brother (Barnes et al., 2018). Additionally, a CRISPR-Cas9-generated *OCRL* knockout (690 KO) iPSC line, previously generated using CRISPR-Cas9 from a healthy, unrelated control (690 Ctrl), was obtained from Herbert Lachman's laboratory and used as an independent model of OCRL deficiency (Barnes et al., 2018). To verify pluripotency, all iPSC lines expressed canonical markers Nanog and Oct4, confirming robust stemness and proliferative capacity (Figure 1a, b). As expected, OCRL protein expression was absent in OCRL knockout iPSCs and markedly reduced in LS100 iPSCs compared to the WT-OCRL control line (LS 200) (Figure 1a, b). Following neuronal induction (Figure 1c), OCRL-deficient iPSCs exhibited altered differentiation patterns compared to control cells. Specifically, we observed an increased proportion of GFAP-positive cells, indicative of astrocytic

identity, in OCRL-deficient cultures relative to controls (Figure 1d, e). To further characterize lineage specification, we performed qPCR analysis of neural markers. Expression of neuronal markers (*FOXG1*, *NEUN*) was higher in control and wild-type iNs (Figure 1f), whereas the astrocytic marker GFAP was significantly upregulated in OCRL knockout and LS-derived iNs (Figure 1g).

## 2.2. OCRL deficiency leads to mitochondrial dysfunction in OCRL knockout and LS-patient-derived iN cells

To investigate whether OCRL deficiency disrupts mitochondrial integrity and bioenergetic function during neuronal differentiation, we assessed mitochondrial activity in OCRL knockout and LS patient-derived iNs generated from iPSCs. Quantitative PCR analysis of mitochondrial DNA (mtDNA) genes *CO2* and *D-LOOP* revealed a marked reduction in mtDNA transcript levels in OCRL-deficient iNs compared to wild-type and sibling control iNs (Figure 2a). Consistently, immunostaining for 8-oxo-dG, a marker of oxidative DNA damage, demonstrated pronounced oxidative stress in OCRL knockout and LS iNs, whereas wild-type and control cells showed minimal reactivity (Figure 2b, c). Because these results suggested impaired mitochondrial oxidative phosphorylation (OXPHOS), we next evaluated mitochondrial respiratory function using Seahorse extracellular flux analysis. The oxygen consumption rate (OCR), a direct measure of OXPHOS efficiency, was significantly reduced in both *OCRL* knockout and LS-derived iNs compared with wild-type and unaffected control iNs (Figure 2d).

## 2.3. Elevated astrocytic differentiation during neuronal differentiation of NSPCs in the Lowe syndrome (IOB) mouse model

Based on our iPSC-based findings, we hypothesized that CNS development in the LS mouse model would exhibit higher levels of astrocytic progenitor cells than neuronal progenitor cells. To examine neural cell composition *in vivo*, we analyzed brain tissue from the humanized Lowe syndrome (IOB) mouse model using adult mice (2-month-old mice), previously characterized for its ocular phenotype (Bothwell et al., 2011). Brain sections were assessed for the expression of neuronal and astrocytic markers (Supplementary Figure 3).

To further assess lineage specification, we quantified the expression of neuronal markers (*PAX6*, *NEUN*) (Figure 3a) and the astrocytic marker *GFAP* (Figure 3b) in the brain tissue. *GFAP* expression was increased in IOB brain tissue compared to wild-type controls, whereas expression of neuronal markers (*PAX6*, *NEUN*) was reduced (Figure 3a, b). Immunohistochemical analysis of brain sections showed an increased GFAP-positive signal relative to neuronal marker staining in IOB mice compared to controls (Figure 3c, d).

## 2.4. Reduced mitochondrial function during CNS development in the LS mouse model

To assess mitochondrial status *in vivo*, we analyzed mitochondrial DNA levels and oxidative stress in brain tissue from 2-month-old IOB mice and age-matched wild-type (WT) controls. Based on our findings from LS patient-derived iNs, we hypothesized that OCRL-deficiency *in vivo* similarly impairs mitochondrial function during CNS development. Quantitative PCR analysis revealed a significant reduction in mitochondrial DNA (mtDNA) measured by the *mito1* and *COX1*, in IOB brain tissues compared with age-matched WT controls (Figure 4a). To evaluate mitochondrial oxidative stress, we performed immunostaining for 8-oxo-dG, a well-established marker of oxidative DNA damage (Hahm et al., 2022). IOB brain sections displayed an increased 8-oxo-dG-positive signal compared to WT controls (Figure 4b, c).

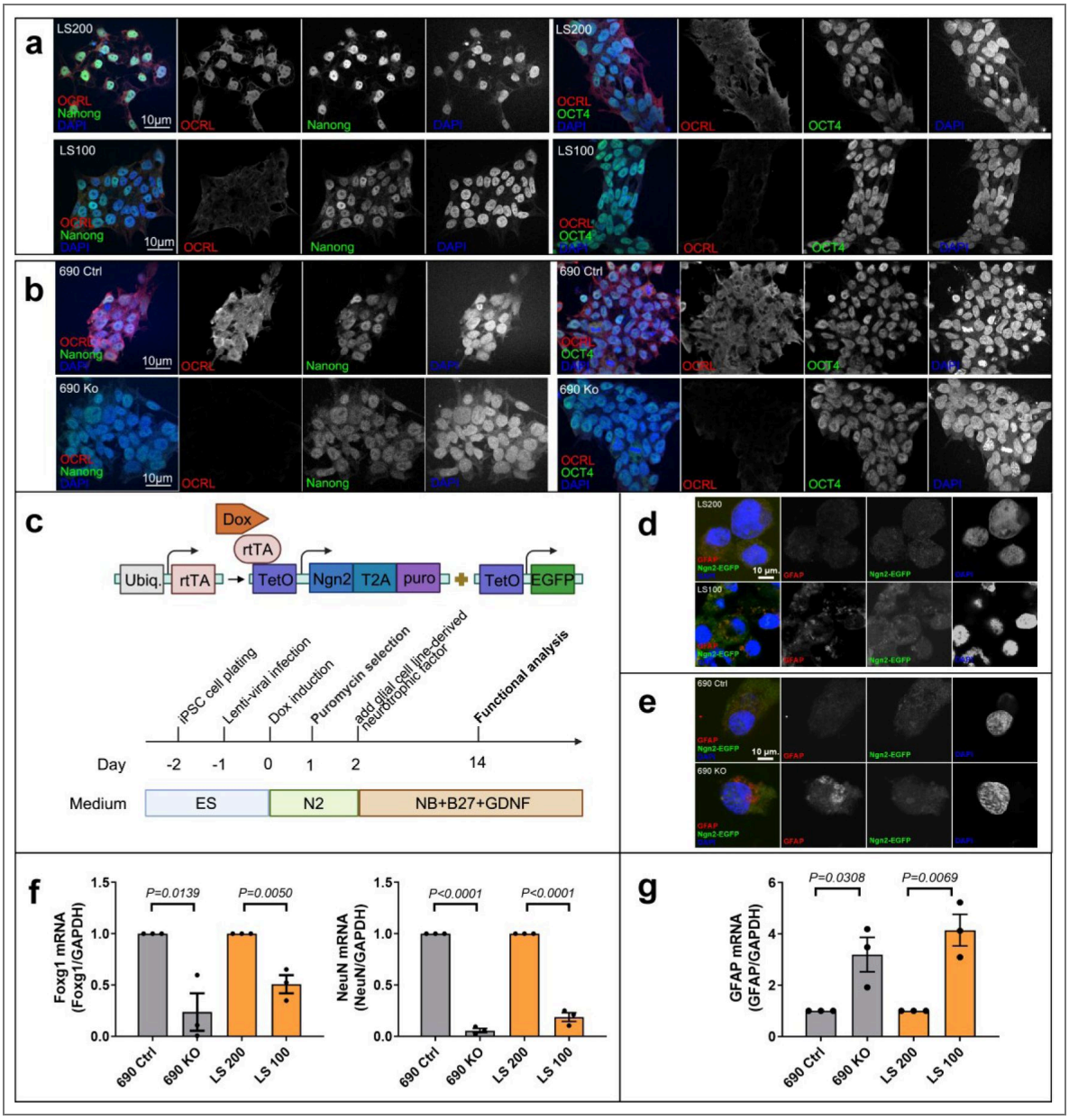


**Figure 1. Increased astrocyte production during neuronal differentiation in OCRL-deficient and Lowe syndrome iPSCs.**

(a and b) Immunofluorescence analysis of OCRL expression and pluripotency markers in iPSCs. Cells were stained for OCRL (red) and pluripotency markers Nanog and OCT4 (green), with nuclei counterstained with DAPI (blue). Scale bars are as indicated. (c) Schematic representation of Ngn2-mediated direct conversion of iPSCs into induced neurons (iNs) using lentiviral vectors (adapted from Zhang et al., 2013). (d and e) Immunofluorescence analysis of iPSC-derived iNs following neuronal induction. Cells were stained for GFAP (red), with Ngn2-EGFP marking transduced cells. Nuclei were counterstained with DAPI (blue). Scale bars as indicated. (f) qPCR analysis of neuronal markers (*FOXG1* and *NEUN*) in iN cells derived from control and OCRL-deficient iPSCs. (g) qPCR analysis of *GFAP* expression in iN cells. Gene expression values were normalized to *GAPDH*. Data represent the mean ± SEM from three independent experiments. Statistical significance was determined using Student's t-test. Changes in gene expression reflect relative marker levels and do not directly quantify cell-type proportions.

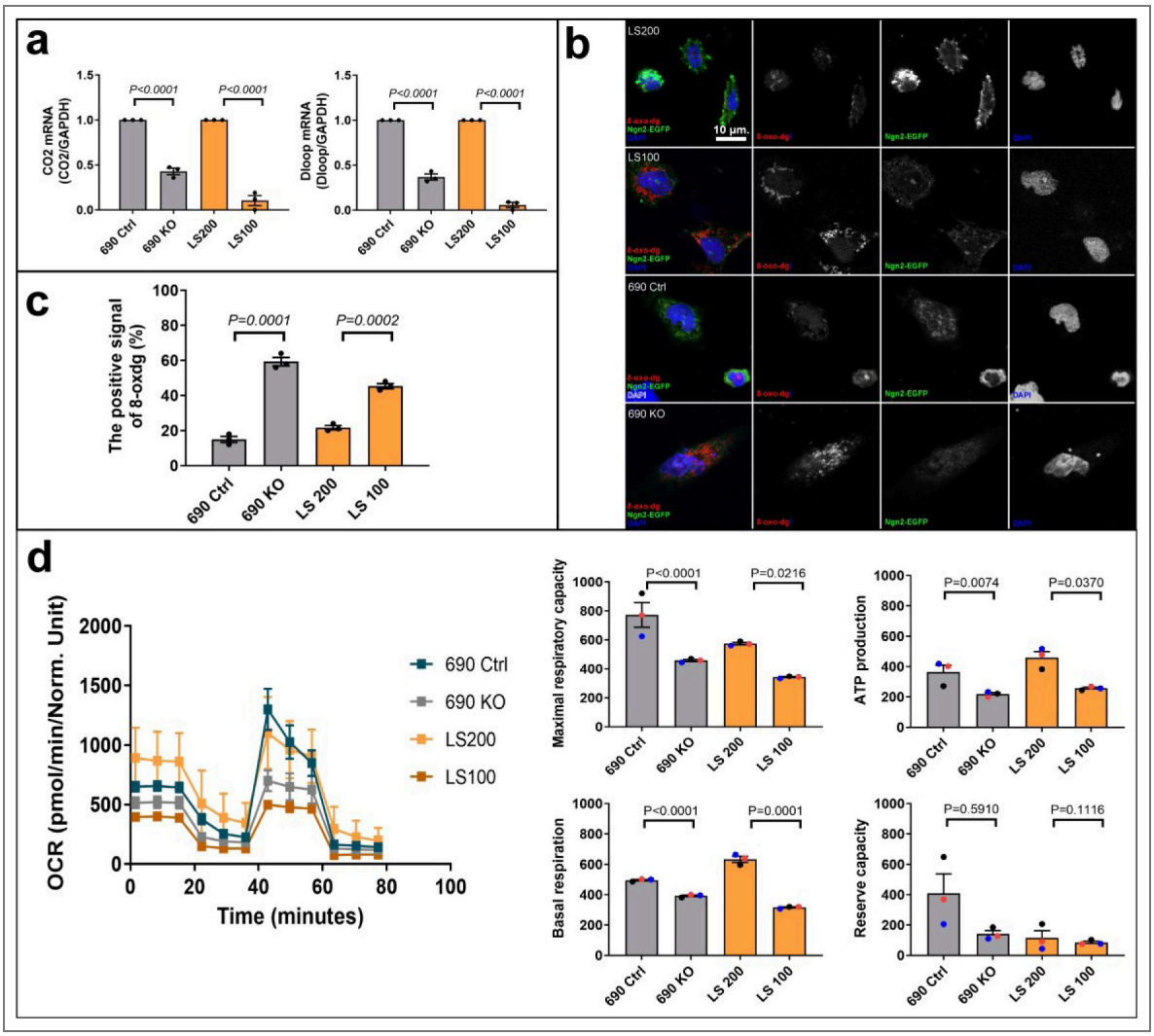


**Figure 2. Altered mitochondrial parameters in OCRL-deficient iPSC-derived neurons**

(a) qPCR analysis of mitochondrial DNA (mtDNA) levels, assessed using *CO2* and *D-loop* regions, in iN cells derived from control and OCRL-deficient iPSCs. (b) Immunofluorescence staining for 8-oxo-dG (red), a marker of oxidative DNA damage, in iN cells. Ngn2-EGFP (green) marks induced neurons. Nuclei are counterstained with DAPI (blue). Scale bars as indicated. (c) Quantification of the percentage of 8-oxo-dG-positive cells. More than 100 cells were analyzed per independent experiment. (d) Mitochondrial respiration was assessed by oxygen consumption rate (OCR) using Seahorse extracellular flux analysis. Gene expression values were normalized to GAPDH. Data represent mean ± SEM from three independent experiments. Statistical significance was determined using Student's t-test.

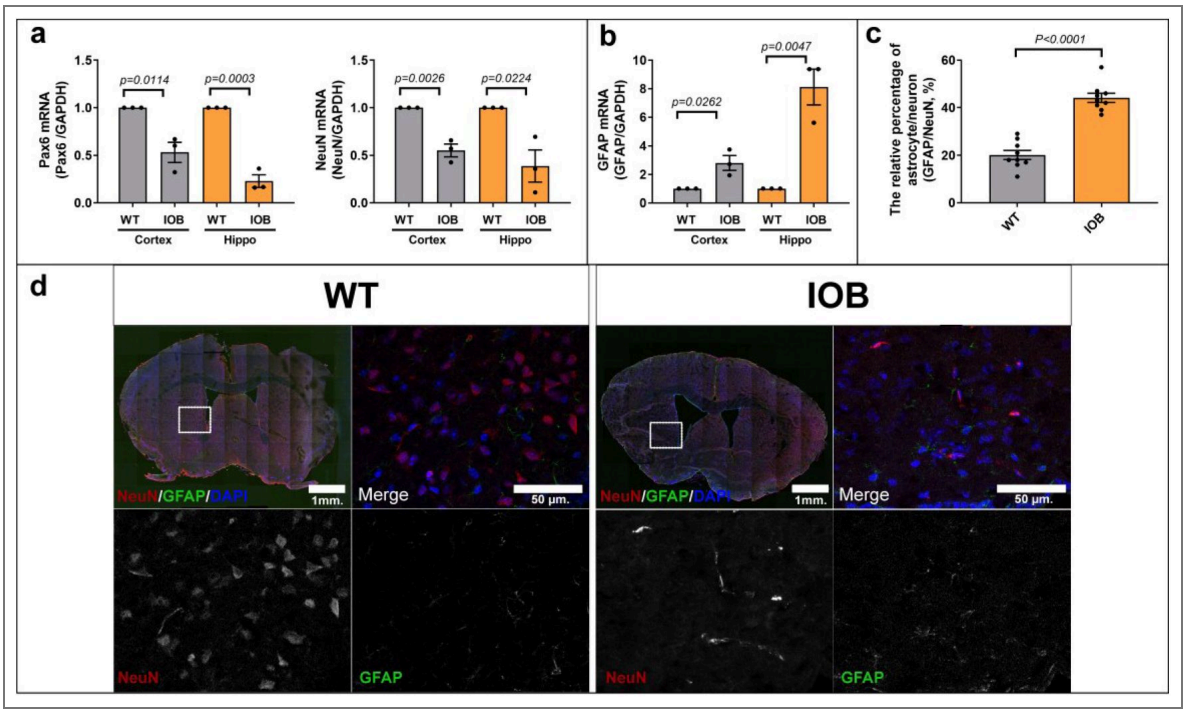


**Figure 3. Altered neuronal and astrocytic marker expression in the Lowe syndrome mouse model**

(a) qPCR analysis of progenitor-associated marker (*Pax6*) and neuronal markers (*NeuN*) in brain tissue. (b) qPCR analysis of astrocytic marker *GFAP* in brain tissue. (c) Quantification of NeuN and GFAP signal intensity in brain sections. More than 100 cells were analyzed per independent experiment. (d) Representative images of brains from wild-type (WT) and *INPP5B/OCRL* double knockout (IOB) mice. Immunofluorescence staining of brain sections for NeuN (red) and GFAP (green). Nuclei are counterstained with DAPI (blue). Scale bars as indicated. Gene expression values were normalized to GAPDH. Data represent mean ± SEM. Statistical significance was determined using Student's t-test.

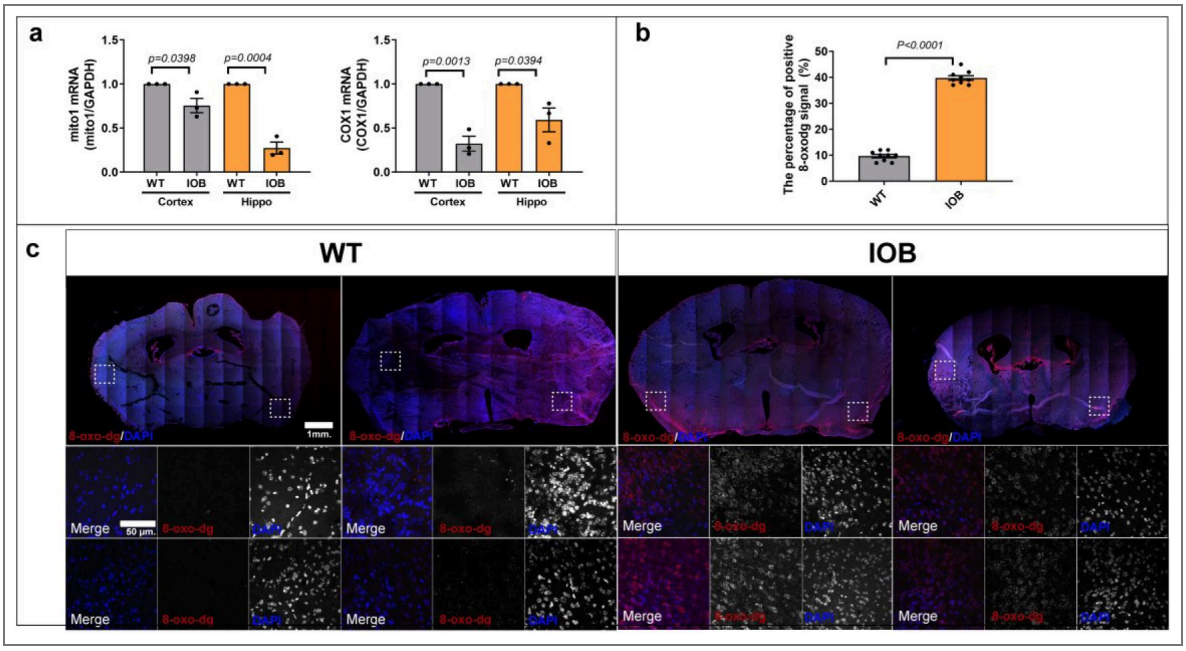


**Figure 4. Altered mitochondrial parameters in the Lowe syndrome mouse brain.**

(a) qPCR analysis of mitochondrial DNA (mtDNA), assessed using *mito1* and *COX1* in brain tissue from WT and IOB mice. (b) Quantification of 8-oxo-dG-positive signal in brain sections. More than 100 cells were analyzed per independent experiment. (c) Immunofluorescence staining for 8-oxo-dG (red) in brain sections. Nuclei are counterstained with DAPI (blue). Scale bars as indicated. Gene expression values were normalized to GAPDH. Data represent mean ± SEM. Statistical significance was determined using Student's t-test.

### 2.5. Altered mitochondrial parameters in OCRL-deficient zebrafish larvae

To assess mitochondrial parameters in an independent *in vivo* model, we analyzed OCRL-deficient zebrafish larvae generated by CRISPR/Cas9-mediated targeting of the zebrafish *ocrl* gene, the homolog of human *OCRL* (Supplementary Figure 4). OCRL-deficient larvae exhibited developmental abnormalities compared to control gRNA-injected larvae (Figure 5a) and showed reduced survival over time (Figure 5b,c). Mitochondrial reactive oxygen species (ROS) were evaluated using MitoSOX staining. OCRL-deficient larvae displayed increased MitoSOX signal in both cranial and ocular regions compared to controls (Figure 5d). Mitochondrial content was assessed by TOM20 immunostaining. OCRL-deficient larvae showed reduced TOM20 signal relative to control larvae (Figure 5e). Mitochondrial membrane potential (ΔΨm) was measured using MitoTracker CMXRos. OCRL-deficient larvae exhibited reduced MitoTracker CMXRos intensity in cranial and ocular regions compared to controls (Figure 5f).

### 2.6. Defective ciliary homeostasis underlies neuronal dysfunction in Lowe syndrome

Given the mitochondrial dysfunction observed in OCRL-deficient models, we hypothesized that defective mitochondrial function may secondarily impair ciliary structure and Shh signaling in LS. To assess Shh pathway activity, we analyzed gene expression in iNs derived from OCRL knockout and LS patient-derived iPSCs. Quantitative PCR analysis revealed a marked downregulation of *GLI1*, *PTCH1*, and *Shh* transcripts in OCRL-deficient iNs compared with wild-type and unaffected sibling control iNs (Figure 6a). Consistently, primary cilia were examined in brain sections from IOB mice. IOB brain sections exhibited a significant reduction in the number of ciliated cells and elongated cilia length compared to wild-type controls (Figure 6b, c). To further assess the impact on Shh signaling *in vivo*, we quantified the mRNA levels of key pathway components, including *Gli1*, *Gli2*, *Gli3*, and *Ptch1*, in IOB and WT brains. All four transcripts were significantly reduced in IOB mice (Figure 6d). Western blot analysis confirmed decreased protein expression of *Shh* and *Gli1* in IOB brains compared to WT (Figure 6e).

## 3. Discussion

In this study, we expand our analysis across multiple model systems, including patient-derived iPSCs, CRISPR knockout human cells, the IOB mouse model, and an independent zebrafish OCRL-deficient model, to identify mitochondrial dysfunction as a conserved phenotype of OCRL loss. Across all models, OCRL loss was consistently associated with reduced mitochondrial DNA levels, decreased oxidative phosphorylation, and increased oxidative stress. In zebrafish, these alterations were further supported by reduced mitochondrial membrane potential, increased mitochondrial ROS, and decreased TOM20 staining, indicating reductions in both mitochondrial function and mitochondrial content. Together, these findings support the role of mitochondrial dysfunction as a contributing cause for OCRL deficiency in Lowe syndrome. Consistent with this, recent studies independently reported mitochondrial dysfunction alongside altered neurodevelopmental trajectories in OCRL-deficient systems, including enhanced Notch-dependent gliogenesis and impaired mitochondrial structure and function (Philip et al., 2025; Sharma et al., 2025). Collectively, these studies support that mitochondrial dysregulation is a conserved feature of neurologic abnormalities in Lowe syndrome. These mitochondrial defects coincided with a consistent shift in lineage specification. Our data showed an altered balance between neuronal and astrocytic differentiation. This distinction supports that OCRL deficiency influences lineage specification rather than completely blocking neuronal development. In line with our observations, Sharma et al. recently showed enhanced Notch-dependent glial differentiation and delayed neuronal maturation in OCRL-deficient models (Sharma et al., 2025). Together, these studies support the concept that OCRL deficiency alters cell-fate decisions during neural

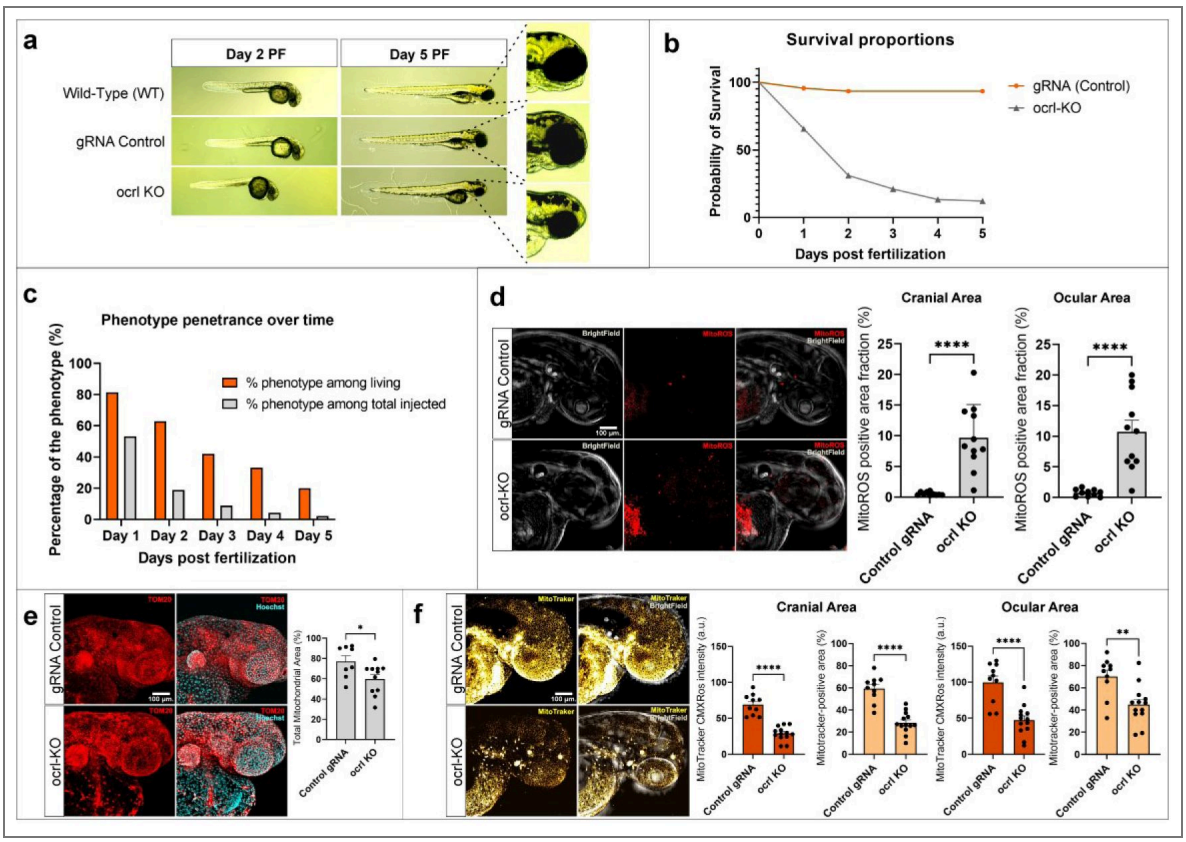


**Figure 5. OCRL loss is associated with mitochondrial dysfunction, oxidative stress, and reduced survival in zebrafish**

(a) Representative brightfield images of zebrafish larvae at 2 and 5 days post-fertilization (dpf), including wild-type (WT), control gRNA-injected, and *ocrl* knockout (KO) groups. (b) Kaplan-Meier survival analysis of zebrafish larvae. OCRL-deficient larvae exhibit reduced survival compared to control gRNA-injected larvae. (c) Quantification of phenotype penetrance over time (1-5 dpf), presented as (i) percentage of affected larvae among living animals and (ii) percentage of affected larvae relative to total injected embryos. (d) Mitochondrial reactive oxygen species (ROS) assessed by MitoSOX staining. Representative images and quantification of MitoSOX-positive area fraction (%) in cranial and ocular regions are shown. (e) Mitochondrial content assessed by TOM20 immunostaining. Representative images and quantification of TOM20-positive area fraction (%) are shown. (f) Mitochondrial membrane potential (ΔΨm) assessed by MitoTracker CMXRos staining. Representative images and quantification of MitoTracker CMXRos intensity (a.u.) and positive area fraction (%) in cranial and ocular regions are shown. Data are presented as mean ± SEM from n = 10-15 larvae per group. Statistical significance was determined using Student's t-test unless otherwise indicated. Imaging and quantification were performed under identical conditions across all groups.

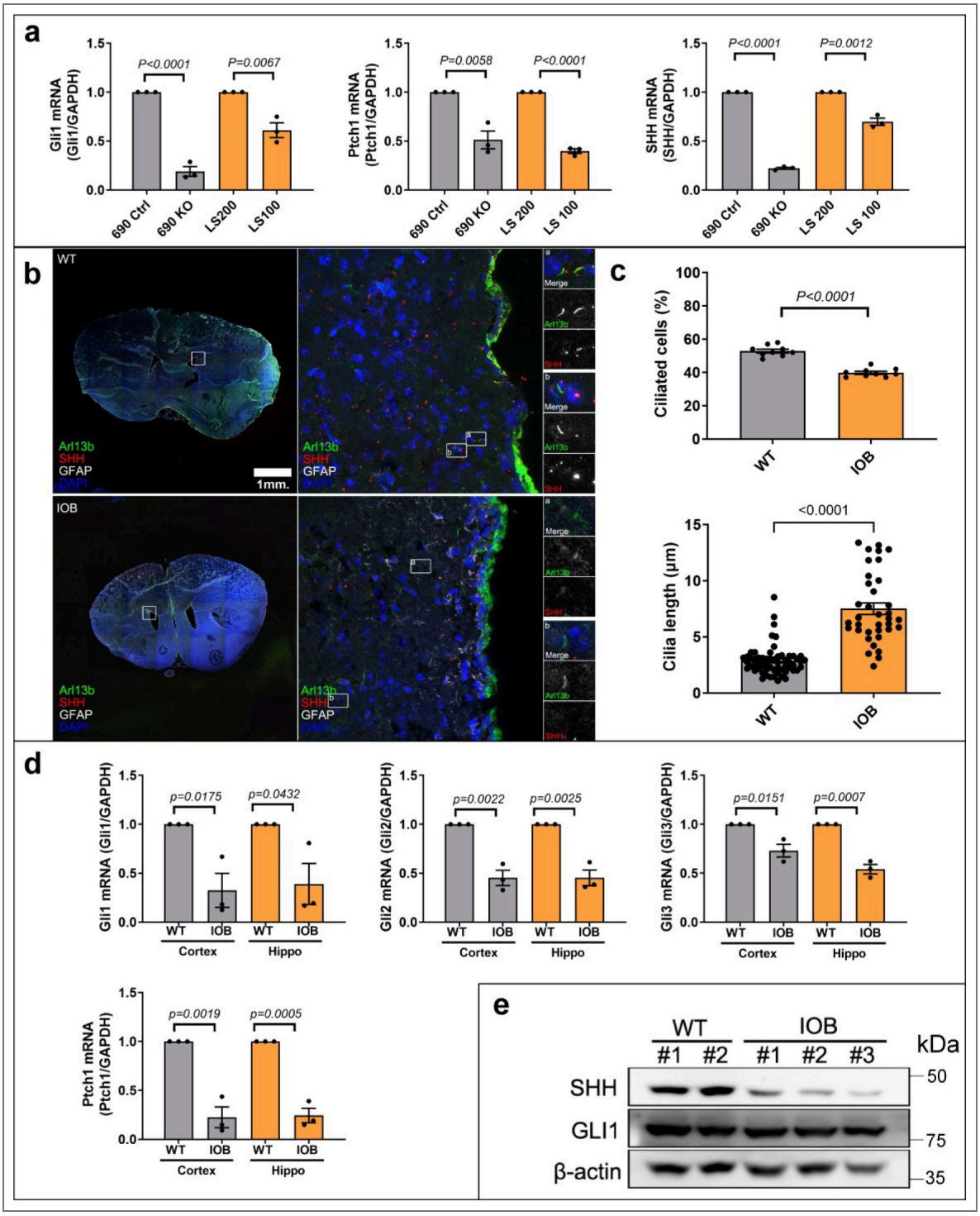


**Figure 6. Altered ciliary parameters and Sonic Hedgehog signaling in OCRL-deficient models**

(a) qPCR analysis of Shh pathway genes (*GLI1*, *PTCH1*, *SHH*) in iPSC-derived iN cells. (b) Immunofluorescence staining of brain sections for SHH (red) and the ciliary marker ARL13B (green). Nuclei are counterstained with DAPI (blue). Scale bars as indicated. (c) Quantification of the ciliated cells and cilia length in brain sections. More than 100 cells were analyzed per independent experiment. (d) qPCR analysis of Hedgehog pathway genes (*Gli1*, *Gli2*, *Gli3*, *Ptch1*) in brain tissue from WT and IOB mice. (e) Western blot analysis of SHH and GLI1 protein levels in brain tissue. β-actin was used as a loading control. Gene expression values were normalized to GAPDH. Data represent mean ± SEM. Statistical significance was determined using Student's t-test.

development. Importantly, our data do not directly address Notch signaling, but instead identify mitochondrial dysfunction and altered ciliary/Shh signaling as additional pathways associated with this phenotype.

In addition to mitochondrial abnormalities, we identified alterations in ciliary homeostasis and Shh signaling. OCRL-deficient models exhibited reduced expression of key Shh pathway components at both the transcript and protein levels. In the IOB mouse brain, this was accompanied by a decreased number of ciliated cells together with increased cilia length, indicating altered ciliary homeostasis. Given the central role of the primary cilium in Shh signal transduction, these findings implicate disrupted ciliary/Shh signaling as an additional feature of OCRL deficiency (Zhuang, 2025). Notably, mitochondrial imbalance was shown to alter cilia length and disrupt cilia-dependent processes *in vivo*, linking bioenergetic state to developmental patterning (Burkhalter et al., 2019; Moruzzi et al., 2022).

Previous studies have reported adaptive ciliary responses to mitochondrial stress, including increased ciliogenesis and ciliary remodeling driven by ROS signaling and transcriptional activation of ciliogenic programs (Ignatenko et al., 2023; Moruzzi et al., 2022). In contrast, OCRL-deficient models in our study exhibited a reduced number of ciliated cells together with altered ciliary morphology, suggesting impaired ciliary homeostasis rather than a compensatory ciliogenic response. This difference may reflect the nature of OCRL deficiency, which represents a chronic disruption of phosphoinositide metabolism and endosomal trafficking rather than an acute mitochondrial stress response (Mehta et al., 2014). Prior studies established zebrafish as a relevant model for Lowe syndrome, revealing defects in neuroepithelial development and endocytic trafficking, including seizure-like phenotypes (Williams et al., 2022). Our findings extend these observations by linking these developmental abnormalities to mitochondrial dysfunction as a potential underlying mechanism. Given the critical role of OCRL in membrane dynamics at the ciliary base, its loss is likely to impair the formation and maintenance of cilia despite the presence of mitochondrial stress signals (Luo et al., 2012). Sustained mitochondrial dysfunction may therefore be associated with defective ciliary signaling rather than adaptive ciliogenesis (Kim et al., 2025; Moruzzi et al., 2022).

Thus, we propose a model in which OCRL deficiency leads to mitochondrial dysfunction and increased oxidative stress, which are associated with alterations in neural lineage balance and disruption of Shh signaling (Figure 7). While the causal relationships between these phenotypes remain to be established, oxidative stress may represent a potential link between mitochondrial impairment and downstream developmental signaling pathways. Shh signaling is a key regulator of neural progenitor fate and astrocyte development and contributes to the maintenance of region-specific astrocyte functions in the central nervous system (Garcia, 2021; Gingrich et al., 2022; Hill et al., 2021, 2019). Given the established roles of astrocytes in synapse formation, maturation, and elimination (Akdemir et al., 2020; Clavreul et al., 2022; Farhy-Tselnicker and Allen, 2018), disruption of these pathways may contribute to the altered neuron-to-astrocyte balance observed in OCRL-deficient systems. Importantly, our findings do not exclude the Notch-dependent mechanism described by Sharma et al. (Sharma et al., 2025), but suggest that mitochondrial dysfunction and altered ciliary/Shh signaling represent additional pathways associated with neurodevelopmental abnormalities in Lowe syndrome.

Several limitations should be considered. The *in vivo* analyses were limited to available brain regions, and astrocytic differentiation was primarily assessed using GFAP expression. Furthermore, while mitochondrial dysfunction, altered neural differentiation, and impaired ciliary/Shh signaling were consistently observed across models, the causal relationships between these phenotypes remain to be determined.

In summary, our findings identify mitochondrial dysfunction and altered ciliary signaling as key features of OCRL deficiency across multiple model systems. By integrating these observations, we propose a conserved mitochondria-ROS-signaling axis associated with altered neural differentiation in Lowe syndrome (Figure 7). This framework highlights mitochondrial

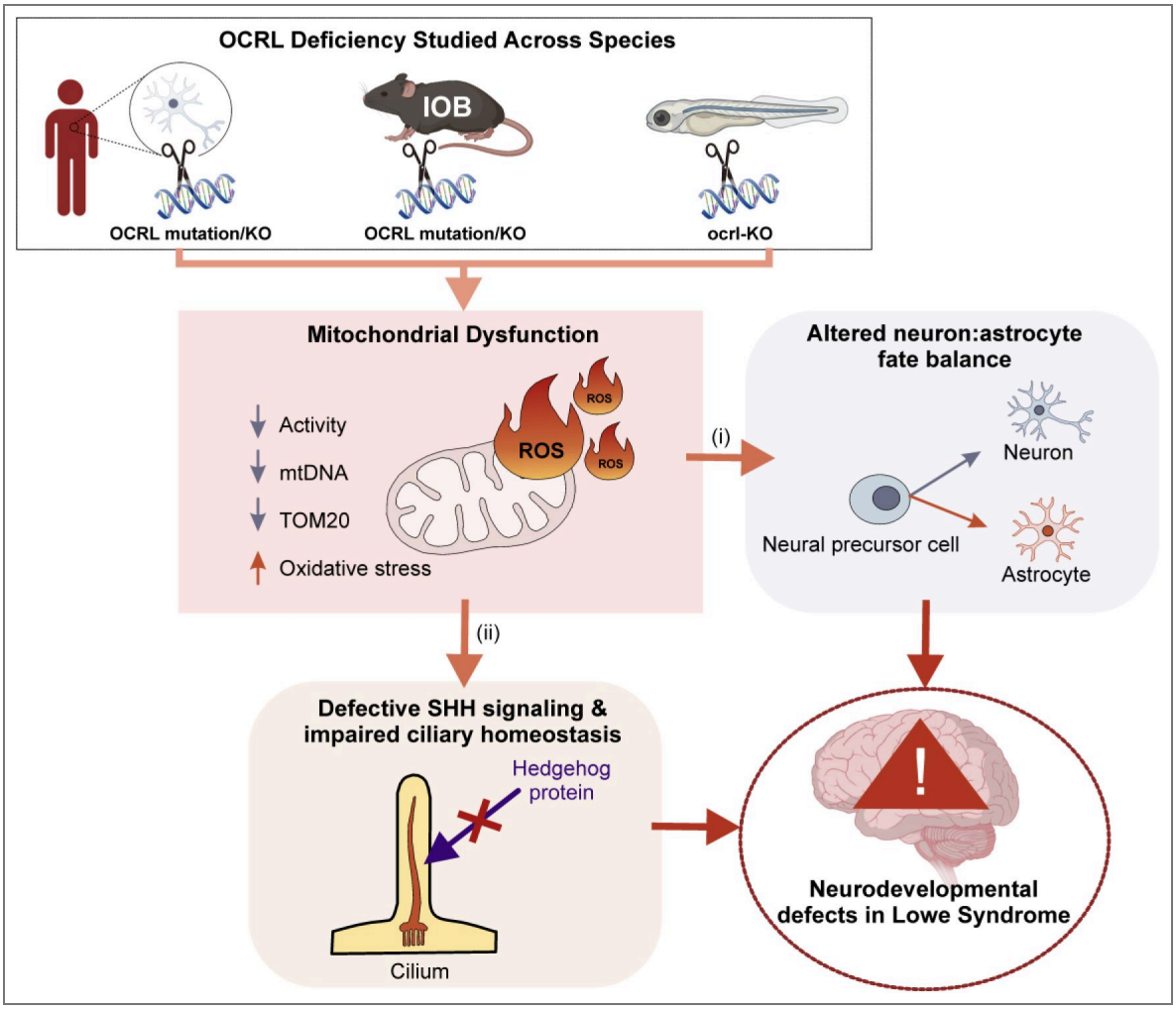


**Figure 7. OCRL deficiency disrupts neuronal development through mitochondrial dysfunction, oxidative stress, and impaired Shh-cilia signaling**

Schematic representation of the integrated findings across experimental systems. OCRL deficiency leads to mitochondrial dysfunction, characterized by reduced mitochondrial DNA, decreased oxidative phosphorylation, reduced mitochondrial content, and increased oxidative stress. Elevated oxidative stress is associated with two parallel processes: (i) altered balance between neuronal and astrocytic cell states and (ii) reduced Shh signaling, accompanied by changes in ciliary parameters, including decreased proportion of ciliated cells and increased cilia length. These combined alterations are associated with impaired neuronal development in Lowe syndrome.

homeostasis and ciliary signaling as interconnected processes in neurodevelopment and suggests that targeting bioenergetic or redox pathways may represent a potential therapeutic avenue in Lowe syndrome.

# 4. Materials and methods

## 4.1. iPSCs culture and reagent

iPSCs were cultured on matrigel (Corning, 354277) in mTeSR1 Plus medium (Stem Cell Technologies, 85850). Media were changed daily, and confluent cells were passaged (1:2) using ReLeSR (Stem Cell Technologies, 05872). All cells were maintained at 37° C, 5% $CO_2$.

## 4.2. Animals

All animal experiments adhered to the guidelines of the Association for Research in Vision and Ophthalmology Statement for the Use of Animals in Ophthalmic and Vision Research and were approved by the Institutional Animal Care and Use Committee (IACUC) of Stanford University School of Medicine.

### 4.2.1. Mice

2-month-old $Ocrl^{-/-}$ $Inpp5b^{-/-}$ $INPP5B^{+/+}$ (IOB) mice were generously provided by Robert L. Nussbaum (University of California, San Francisco). Wild-type (C57BL/6) mice from the Jackson Laboratories were used as controls for the IOB mice. The animals were housed under a 12-hour light/dark cycle with free access to water and food. Mice were anesthetized with isoflurane, with oxygen flow set to 2 liters per minute and isoflurane at 1% delivered via a nose cone.

### 4.2.2. Zebrafish husbandry and generation of OCRL-deficient zebrafish larvae

Wild-type zebrafish (Danio rerio) were maintained under standard conditions at 28.5 °C on a 14 h light / 10 h dark cycle. Embryos were obtained by natural mating and raised in E3 embryo medium. All procedures were conducted in accordance with institutional animal care guidelines and approved protocols.

OCRL-deficient zebrafish were generated using CRISPR/Cas9-mediated gene disruption targeting the zebrafish *ocrl* ortholog. The zebrafish experimental procedures were adapted from a previously established protocol (Pagán et al., 2022). Briefly, guide RNAs (gRNAs) were designed to target coding regions of *ocrl* using CRISPR design tools. Synthetic crRNA and tracrRNA (IDT) were complexed with recombinant Cas9 protein (IDT, Alt-R Cas9 V3) to form ribonucleoprotein (RNP) complexes. The RNP complex was prepared as follows: the crRNA:tracrRNA duplex was annealed at 95°C for 5 minutes and cooled to room temperature, then incubated with Cas9 protein for 10-15 minutes at room temperature. Approximately 1-2 nL of RNP complex was microinjected into one-cell-stage zebrafish embryos using a microinjection system. As a control, embryos were injected with a non-targeting gRNA (out-of-genome control) to account for CRISPR-associated toxicity. Injected embryos were maintained at 28.5 °C and screened for phenotypic abnormalities and survival. Larval survival was monitored daily from 1 to 5 days post-fertilization (dpf). Dead larvae were removed at each time point. Developmental phenotypes were assessed by brightfield imaging using a stereomicroscope, with particular attention to body morphology, cranial structure, and eye development.

## 4.3. Zebrafish mitochondrial assays (MitoSOX, MitoTracker CMXRos, and TOM20 staining)

Mitochondrial function, reactive oxygen species (ROS), and mitochondrial content were assessed in OCRL-deficient zebrafish larvae at 2 days post-fertilization (2 dpf). To assess mitochondrial membrane potential (ΔΨm) and mitochondrial ROS, live zebrafish larvae were stained with MitoTracker™ Red CMXRos (Thermo Fisher Scientific) and MitoSOX™ Red (Thermo Fisher Scientific). Larvae at 2 dpf were incubated in E3 medium containing 100 nM MitoTracker CMXRos and 2 μM MitoSOX for 20 minutes at 28.5 °C in the dark. Following incubation, larvae were washed

twice in fresh E3 medium to remove excess dye, anesthetized using tricaine (MS-222), and mounted in low-melting-point agarose in a confocal imaging dish. Fluorescent images were acquired using an Olympus fluorescence microscopy system under identical acquisition settings across experimental groups. Quantification was performed using Fiji/ImageJ by measuring mean fluorescence intensity or positive area fraction (%) within defined regions of interest (ROIs) corresponding to cranial and ocular regions. For each larva, cranial and ocular regions were analyzed as predefined ROIs. Mitochondrial content was quantified as TOM20-positive area fraction (%) using Fiji/ImageJ. N = 10-15 larvae per group were analyzed.

## 4.4. Plasmids

The lentiviral vectors for Ngn2-mediated conversion of iPSCs to iN cells are from Thomas C. Sudhof's lab (Zhang et al., 2013).

## 4.5. Lentivirus production and infection

$5\times10^5$ 293FT cells were plated on 60-mm dishes using TurboFect™ Transfection Reagent with the following plasmids: 1.5 µg of V-SVG, 2.5 µg of pCMV-gag-pol, and 3.5 µg of the lentiviral vector DNA constructs. The supernatant containing viral particles was harvested 48 h after transfection. Virus-containing media was passed through a 0.45µm filter (Fisher Scientific, 13-100-105).

## 4.6. Generation of iN Cells from Human iPSCs

iN cells were generated using an established Ngn2-based direct conversion protocol (Zhang et al., 2013). iPSCs were treated with Accutase (Stem Cell Technologies, 07920) and plated as dissociated cells in 24-well plates (iPSCs: 1.5 x $10^4$ cells/well) on day 2 (Figure 1c). Cells were plated on matrigel (Corning, 354277)-coated coverslips in mTeSR1 medium. On day 1, lentivirus prepared as described above (0.3 ml/well of 24-well plate) was added to fresh mTeSR1 medium containing polybrene (8 mg/mL, Sigma). On day 0, the culture medium was replaced with DMEM/F12 (Thermo Fisher Scientific, 11-330-057) containing N2(STEMCELL Technologies, 07152), NEAA (Thermo Fisher Scientific, 11-140-050), human BDNF (10 mg/L, STEMCELL Technologies, 78058), human NT-3 (10 mg/L, PeproTech, 450-03), and mouse laminin (0.2 mg/L, Thermo Fisher Scientific, 23017015). Doxycycline (2 g/L, Fisher Scientific, AC446060050) was added on day 0 to induce TetO gene expression and retained in the medium until the end of the experiment. On day 1, a 24 hr puromycin selection (1 mg/L) period was started. On day 2, replace with Neurobasal medium (Thermo Fisher Scientific, 21103049) supplemented with B27/Glutamax (Invitrogen) containing BDNF and NT3. After day 2, 50% of the medium in each well was exchanged every 2 days. FBS (2.5%) was added to the culture medium on day 10 to support astrocyte viability, and iN cells were assayed on day 14 or 21 in most experiments.

## 4.7. Immunostaining

### 4.7.1. Cell immunostaining

Cells were cultured on coverslips coated with 0.1 mg/mL poly-L-lysine and fixed with methanol at -20°C for 15 minutes. The cells were then washed three times with PBS and incubated in a blocking buffer containing 3% bovine serum albumin (w/v) and 0.1% Triton X-100 in PBS for 30 minutes at room temperature (RT). Primary antibodies, diluted in the blocking buffer, were applied for 2 hours at RT. Alexa Fluor 488-, 594-, or 647-conjugated goat secondary antibodies (Thermo Fisher Scientific) were used at a 1:500 dilution and incubated for 1 hour at RT. DNA was stained with 4,6-diamidino-2-phenylindole (DAPI; Thermo Fisher Scientific). Coverslips were then mounted on slides using ProLong™ Gold Antifade mounting medium (Thermo Fisher Scientific).

### 4.7.2. Brain section immunostaining

Mouse brains were harvested and fixed in 4% paraformaldehyde (PFA) at 4°C, followed by cryoprotection in sucrose solution (e.g., 30% sucrose in PBS). Brains were embedded in optimal cutting temperature (OCT) compound and sectioned using a cryostat to obtain 20 µm sections. Brain sections were permeabilized in 0.3-0.5% Triton X-100 in PBS for 20-30 minutes and blocked

in 5% BSA and 0.1% Triton X-100 in PBS for 1 hour at RT. Sections were incubated with primary antibodies diluted in blocking buffer overnight at 4°C. After washing, sections were incubated with appropriate Alexa Fluor-conjugated secondary antibodies (1:500) for 1 hour at RT. Nuclei were stained with DAPI. Sections were mounted using an antifade mounting medium and imaged using a confocal microscope under identical acquisition settings across samples.

### 4.7.3. Zebrafish whole-mount immunostaining

For whole-mount staining, zebrafish larvae at 2 dpf were fixed in 4% PFA overnight at 4°C, washed in PBS, and permeabilized with 0.5% Triton X-100 in PBS for 30 minutes. Blocking was performed in 5% BSA and 0.1% Triton X-100 in PBS for 1 hour at RT. Larvae were incubated with primary antibodies (e.g., anti-TOM20, 1:200) overnight at 4°C, followed by washing and incubation with Alexa Fluor-conjugated secondary antibodies (1:500) for 1 hour at RT. Samples were mounted in low-melting-point agarose for imaging.

### 4.7.4. Imaging

Fluorescent images were acquired using a Zeiss LSM880 confocal microscope or an Olympus fluorescence microscope, depending on the experimental setup. All images were acquired using identical settings across experimental groups. Image processing and quantification were performed using ZEN software (Carl Zeiss) or Fiji/ImageJ (NIH)

## 4.8. Immunoblotting

Cells were washed twice with ice-cold PBS and lysed in ice-cold RIPA lysis buffer (Millipore, 20-188) containing a protease inhibitor cocktail (Thermo Fisher Scientific, PI78430). The lysate was centrifuged at 13,500 g for 15 minutes at 4°C to remove cell debris. Protein concentrations were measured using the BCA Protein Assay (Thermo Fisher Scientific, 23227). Equal amounts of protein were combined with SDS sample buffer, boiled at 95°C for 5 minutes, and separated by SDS-PAGE. The proteins were then transferred to 0.2 µm nitrocellulose membranes (Bio-Rad, 1620097). The membranes were blocked for 1 hour at room temperature (RT) with 5% non-fat milk in TBS-T (20 mM Tris, pH 7.6, 137 mM NaCl, and 0.1% Tween-20) and incubated overnight at 4°C with primary antibodies in the blocking solution. The membranes were washed three times with TBS-T and incubated with HRP-conjugated anti-mouse or anti-rabbit secondary antibodies (Invitrogen, 31430 and 31460) for 1 hour at RT. After three additional washes with TBS-T, the proteins were visualized using ECL Western blotting substrate (Thermo Fisher Scientific, 34095).

## 4.9. Primary antibodies

Primary antibodies were obtained from the following sources and used according to the manufacturers' instructions: mouse IgG1 anti-OCRL/INPP5b, NeuroMab clone N166A/26 (IF 1: 250; UC Davis/NIH NeuroMab Facility), rabbit anti-Nanog (IF 1: 250; 3580S, Cell Signaling Technology), rabbit anti-Oct-4A (C30A3) (IF 1: 250; 2840S, Cell Signaling Technology), Chicken anti-GFAP(IF 1: 250; ab4674, Abcam), mouse IgG2b anti-8-oxo-Dg (IF 1: 250; 4354-MC-050; R&D systems), rabbit anti-Sonic Hedgehog antibody [EP1190Y] (IF: 1:200; WB: 1:500: ab53281, Abcam), rabbit anti-Gli1 antibody (WB: 1:500: ab217326, Abcam), mouse anti-Arl13b antibody (N295B/66) (IF: 1:500; 75-287, Antibodies Incorporated), mouse anti-NeuN Antibody, clone A60 (IF: 1:200; MAB377, Sigma-Aldrich), mouse anti-β actin (WB: 1:5000: 66009-1, Proteintech), mouse anti-TOM20 (IF 1:200; ab56783, Abcam)

## 4.10. Quantitative real-time PCR (qPCR)

Quantitative real-time PCR (qPCR) was conducted using HiScript III RT SuperMix for qPCR plus gDNA wiper (Vazyme, R323-01). qPCR was performed using FastSYBR Mixture (2X) (CWBio, CW0955L). The amplification was carried out in 20 µl reaction mixtures containing 100 ng of total DNA, 1X SYBR-Green PCR Master Mix, and 0.5 µM of each primer. Each marker was tested in triplicate reactions in a 96-well plate using a three-step amplification protocol: initial denaturation at 95°C for 5 minutes, followed by 40 cycles of 95°C for 15 seconds, 60°C for 30 seconds, and 72°C for 30 seconds. Relative gene expression was calculated using the comparative Ct (ΔΔCt) method

and normalized to GAPDH as an internal control. Each sample was analyzed in triplicate, and no-template controls were included. The sequences of each gene were shown in Supplemental Figures 1 and 2.

### 4.11. Oxygen consumption rate (OCR)

Oxygen consumption rate (OCR) was measured using a Seahorse Biosciences XFe96 extracellular flux analyzer. Cells were seeded at a density of $1.25 \times 10^5$ cells per well in XFe96 cell culture plates. After 24 hours, cell attachment was confirmed, and the cells were incubated overnight at 37°C with 5% CO2. Prior to the assay, the cells were switched to Seahorse XF DMEM medium containing 1 mM pyruvate, 2 mM glutamine, and 10 mM glucose and equilibrated for 1 hour at 37°C without CO2. OCR was then measured using the following inhibitors: 2.5 μM oligomycin, 2 μM carbonyl cyanide 4-(trifluoromethoxy) phenylhydrazone (FCCP), and 0.5 μM rotenone combined with 0.5 μM antimycin A (Agilent Technologies, 103015-100). Each condition was tested in triplicate cycles, consisting of 3 minutes of mixing followed by 3 minutes of measurement. After the assay, the cell number per well was determined using the Cytation 5, and the OCR was normalized to the cell number for each well.

### 4.12. Primary cilia quantification

Primary cilia were visualized by immunostaining using ARL13B as a ciliary marker. Images were acquired using a confocal microscope under identical acquisition settings across all samples. The proportion of ciliated cells was quantified by manually counting ARL13B-positive cilia relative to total nuclei (DAPI) within defined regions of interest (ROIs). Cilia length was measured manually using Fiji/ImageJ. For each cilium, a line was drawn along the length of the ARL13B-positive structure using the segmented line tool, and the length was recorded in micrometers (μm) after spatial calibration. All measurements were performed using identical thresholding and analysis settings across groups.

### 4.13. Statistical data analysis

All data are presented as the mean with standard deviation (SD) from at least 3 independent experiments. Experimental samples and numbers for statistical testing are reported in the corresponding figure legends. All p-values are from Student's t-tests for two-group comparisons (GraphPad Prism 8).

## Data availability

All data generated or analyzed during this study are included in the manuscript and supporting files. Source data files containing the numerical data used to generate the figures will be provided with the submission. Additional information is available from the corresponding author upon reasonable request.

## Acknowledgements

We thank Dr. Robert L. Nussbaum (University of California, San Francisco) for generously sharing the IOB mouse strain. We thank Dr. Herbert M. Lachman's lab for the iPSCs of LS.

## Additional information

### Author Contributions

GW, SC, and C-HL designed and carried out the experiments, data analysis, and wrote the manuscript. SC, ZL, JZ, and BL contributed to the manuscript editing and experiment assistance. TK and BW contributed to setting up iPSCs processing. BW and QW contributed to setting up the IOB mouse processing. YS supervised the project.

## Ethics Statement

All animal experiments followed the guidelines of the Association for Research in Vision and Ophthalmology Statement for the Use of Animals in Ophthalmic and Vision Research and were approved by the Institutional Animal Care and Use Committee (IACUC) of Stanford University School of Medicine.

## Funding Statement

This work was supported by RO1-EY32159 (YS), EY-034932 (YS), R01-EY025295 (Y.S.), and an unrestricted grant from Research to Prevent Blindness, New York, NY. VA merit CX001481 (Y.S.), Ziegler Foundation for the Blind (Y.S.), and Children's Health Research Institute Award (Y.S.). Research for Prevention of Blindness Unrestricted grant and NIH P30EY026877 (Stanford Ophthalmology) and R38EY037090 (Stanford Ophthalmology).

## Funding

| Funder | Grant reference number | Author |
|---|---|---|
| HHS \| NIH \| National Eye Institute (NEI) | RO1-EY32159 | Yang Sun |
| HHS \| NIH \| National Eye Institute (NEI) | EY-034932 | Yang Sun |
| HHS \| NIH \| National Eye Institute (NEI) | R01-EY025295 | Yang Sun |
| HHS \| NIH \| National Eye Institute (NEI) | P30EY026877 | Yang Sun |
| HHS \| NIH \| National Eye Institute (NEI) | R38EY037090 | Yang Sun |
| Research to Prevent Blindness (RPB) | | Yang Sun |
| Veterans Administration, Palo Alto Medical Center | BX00638 | Yang Sun |
| Veterans Administration, Palo Alto Medical Center | CX001481 | Yang Sun |

## Author ORCID iDs

**Jingyu Zhao**: https://orcid.org/0009-0000-0989-6593
**Zhiquan Liu**: https://orcid.org/0000-0001-5433-5656
**Yang Sun**: https://orcid.org/0000-0002-5331-0358

# Additional files

***supplement materials***

# References

**Adusumilli VS,** Walker TL, Overall RW, Klatt GM, Zeidan SA, Zocher S, Kirova DG, Ntitsias K, Fischer TJ, Sykes AM, *et al.* (2021) ROS Dynamics Delineate Functional States of Hippocampal Neural Stem Cells and Link to Their Activity-Dependent Exit from Quiescence. *Cell Stem Cell* **28**:300-314.e6. https://doi.org/10.1016/j.stem.2020.10.019 | PubMed

**Akdemir ES,** Huang AY-S, Deneen B (2020) Astrocytogenesis: where, when, and how. *F1000Research* **9** https://doi.org/10.12688/f1000research.22405.1 | PubMed

**Barnes J,** Salas F, Mokhtari R, Dolstra H, Pedrosa E, Lachman HM (2018) Modeling the neuropsychiatric manifestations of Lowe syndrome using induced pluripotent stem cells: defective F-actin polymerization and WAVE-1 expression in neuronal cells. *Molecular Autism* **9**:44 https://doi.org/10.1186/s13229-018-0227-3 | PubMed

**Bökenkamp A,** Ludwig M (2016) The oculocerebrorenal syndrome of Lowe: an update. *Pediatric Nephrology* **31**:2201-2212 https://doi.org/10.1007/s00467-016-3343-3 | PubMed

**Bothwell SP,** Chan E, Bernardini IM, Kuo Y-M, Gahl WA, Nussbaum RL (2011) Mouse model for Lowe syndrome/Dent Disease 2 renal tubulopathy. *Journal of the American Society of Nephrology: JASN* **22**:443-448 https://doi.org/10.1681/ASN.2010050565 | PubMed

**Burkhalter MD,** Sridhar A, Sampaio P, Jacinto R, Burczyk MS, Donow C, Angenendt M, Competence Network for Congenital Heart Defects Investigators, Hempel M, Walther P, *et al.* (2019) Imbalanced mitochondrial function provokes heterotaxy via aberrant ciliogenesis. *The Journal of Clinical Investigation* **129**:2841-2855 https://doi.org/10.1172/JCI98890 | PubMed

**Cabezas R,** Avila M, Gonzalez J, El-Bachá RS, Báez E, García-Segura LM, Jurado Coronel JC, Capani F, Cardona-Gomez GP, Barreto GE (2014) Astrocytic modulation of blood brain barrier: perspectives on Parkinson's disease. *Frontiers in Cellular Neuroscience* **8**:211 https://doi.org/10.3389/fncel.2014.00211 | PubMed

**Clavreul S,** Dumas L, Loulier K (2022) Astrocyte development in the cerebral cortex: Complexity of their origin, genesis, and maturation. *Frontiers in Neuroscience* **16**:916055 https://doi.org/10.3389/fnins.2022.916055 | PubMed

**Craigen WJ,** Graham BH, Wong L-J, Scaglia F, Lewis RA, Bonnen PE (2013) Exome sequencing of a patient with suspected mitochondrial disease reveals a likely multigenic etiology. *BMC medical genetics* **14**:83 https://doi.org/10.1186/1471-2350-14-83 | PubMed

**Dumic KK,** Anticevic D, Petrinovic-Doresic J, Zigman T, Zarković K, Rokic F, Vugrek O (2020) Lowe syndrome - Old and new evidence of secondary mitochondrial dysfunction. *European Journal of Medical Genetics* **63**:104022 https://doi.org/10.1016/j.ejmg.2020.104022 | PubMed

**Escartin C,** Galea E, Lakatos A, O'Callaghan JP, Petzold GC, Serrano-Pozo A, Steinhäuser C, Volterra A, Carmignoto G, Agarwal A, *et al.* (2021) Reactive astrocyte nomenclature, definitions, and future directions. *Nature Neuroscience* **24**:312-325 https://doi.org/10.1038/s41593-020-00783-4 | PubMed

**Farhy-Tselnicker I,** Allen NJ (2018) Astrocytes, neurons, synapses: a tripartite view on cortical circuit development. *Neural Development* **13**:7 https://doi.org/10.1186/s13064-018-0104-y | PubMed

**Garcia ADR** (2021) New Tricks for an Old (Hedge)Hog: Sonic Hedgehog Regulation of Astrocyte Function. *Cells* **10**:1353 https://doi.org/10.3390/cells10061353 | PubMed

**Gingrich EC,** Case K, Garcia ADR (2022) A subpopulation of astrocyte progenitors defined by Sonic hedgehog signaling. *Neural Development* **17**:2 https://doi.org/10.1186/s13064-021-00158-w | PubMed

**Hahm JY,** Park J, Jang E-S, Chi SW (2022) 8-Oxoguanine: from oxidative damage to epigenetic and epitranscriptional modification. *Experimental & Molecular Medicine* **54**:1626-1642 https://doi.org/10.1038/s12276-022-00822-z | PubMed

**Hill SA,** Blaeser AS, Coley AA, Xie Y, Shepard KA, Harwell CC, Gao W-J, Garcia ADR (2019) Sonic hedgehog signaling in astrocytes mediates cell type-specific synaptic organization. *eLife* **8**:e45545 https://doi.org/10.7554/eLife.45545 | PubMed

**Hill SA,** Fu M, Garcia ADR (2021) Sonic hedgehog signaling in astrocytes. *Cellular and molecular life sciences: CMLS* **78**:1393-1403 https://doi.org/10.1007/s00018-020-03668-8 | PubMed

**Ignatenko O,** Chilov D, Paetau I, de Miguel E, Jackson CB, Capin G, Paetau A, Terzioglu M, Euro L, Suomalainen A (2018) Loss of mtDNA activates astrocytes and leads to spongiotic encephalopathy. *Nature Communications* **9**:70 https://doi.org/10.1038/s41467-017-01859-9 | PubMed

**Ignatenko O,** Malinen S, Rybas S, Vihinen H, Nikkanen J, Kononov A, Jokitalo ES, Ince-Dunn G, Suomalainen A (2023) Mitochondrial dysfunction compromises ciliary homeostasis in astrocytes. *The Journal of Cell Biology* **222**:e202203019 https://doi.org/10.1083/jcb.202203019 | PubMed

**Kim JB,** Kim YH, Kim SH, Hyung H, So JH, Park D, Park NY, Choi DK, Bae J-E, Cho D-H (2025) Disrupting mitochondrial β-oxidation by depletion of HADHA impairs primary ciliogenesis. *Scientific Reports* **15**:36544 https://doi.org/10.1038/s41598-025-18451-7 | PubMed

**Lewis RA,** Nussbaum RL, Brewer ED (1993) Lowe Syndrome. In: Adam MP, Feldman J, Mirzaa GM, Pagon RA, Wallace SE, Bean LJ, Gripp KW, Amemiya A (Eds). *GeneReviews®*. Seattle: University of Washington. PubMed

**Luo N,** West CC, Murga-Zamalloa CA, Sun L, Anderson RM, Wells CD, Weinreb RN, Travers JB, Khanna H, Sun Y (2012) OCRL localizes to the primary cilium: a new role for cilia in Lowe syndrome. *Human Molecular Genetics* **21**:3333-3344 https://doi.org/10.1093/hmg/dds163 | PubMed

**Luscher A,** Fröhlich F, Barisch C, Littlewood C, Metcalfe J, Leuba F, Palma A, Pirruccello M, Cesareni G, Stagi M, *et al.* (2019) Lowe syndrome-linked endocytic adaptors direct membrane cycling kinetics with OCRL in Dictyostelium discoideum. *Molecular Biology of the Cell* **30**:2268-2282 https://doi.org/10.1091/mbc.E18-08-0510 | PubMed

**Matusova Z,** Hol EM, Pekny M, Kubista M, Valihrach L (2023) Reactive astrogliosis in the era of single-cell transcriptomics. *Frontiers in Cellular Neuroscience* **17**:1173200 https://doi.org/10.3389/fncel.2023.1173200 | PubMed

**McNeill J,** Rudyk C, Hildebrand ME, Salmaso N (2021) Ion Channels and Electrophysiological Properties of Astrocytes: Implications for Emergent Stimulation Technologies. *Frontiers in Cellular Neuroscience* **15**:644126 https://doi.org/10.3389/fncel.2021.644126 | PubMed

**Mehta ZB,** Pietka G, Lowe M (2014) The Cellular and Physiological Functions of the Lowe Syndrome Protein OCRL1. *Traffic* **15**:471-487 https://doi.org/10.1111/tra.12160 | PubMed

**Moruzzi N,** Valladolid-Acebes I, Kannabiran SA, Bulgaro S, Burtscher I, Leibiger B, Leibiger IB, Berggren P-O, Brismar K (2022) Mitochondrial impairment and intracellular reactive oxygen species alter primary cilia morphology. *Life Science Alliance* **5**:e202201505 https://doi.org/10.26508/lsa.202201505 | PubMed

**Oksanen M,** Lehtonen S, Jaronen M, Goldsteins G, Hämäläinen RH, Koistinaho J (2019) Astrocyte alterations in neurodegenerative pathologies and their modeling in human induced pluripotent stem cell platforms. *Cellular and molecular life sciences: CMLS* **76**:2739-2760 https://doi.org/10.1007/s00018-019-03111-7 | PubMed

**Pagán AJ,** Lee LJ, Edwards-Hicks J, Moens CB, Tobin DM, Busch-Nentwich EM, Pearce EL, Ramakrishnan L (2022) mTOR-regulated mitochondrial metabolism limits mycobacterium-induced cytotoxicity. *Cell* **185**:3720-3738.e13. https://doi.org/10.1016/j.cell.2022.08.018 | PubMed

**Philip RG,** Bhatia P, Sharma Y, Raghu P (2025) Mitochondrial structure and function in OCRL depleted cells. *Frontiers in Cell and Developmental Biology* **13** https://doi.org/10.3389/fcell.2025.1679675 | PubMed

**Pociūtė A,** Pivoriūnas A, Verkhratsky A (2024) Astrocytes dynamically regulate the blood-brain barrier in the healthy brain. *Neural Regeneration Research* **19**:709-710 https://doi.org/10.4103/1673-5374.382248 | PubMed

**Prosseda PP,** Luo N, Wang B, Alvarado JA, Hu Y, Sun Y (2017) Loss of OCRL increases ciliary PI(4,5)P2 in Lowe oculocerebrorenal syndrome. *Journal of Cell Science* **130**:3447-3454 https://doi.org/10.1242/jcs.200857 | PubMed

**Sakakibara N,** Ijuin T, Horinouchi T, Yamamura T, Nagano C, Okada E, Ishiko S, Aoto Y, Rossanti R, Ninchoji T, *et al.* (2022) Identification of novel OCRL isoforms associated with phenotypic differences between Dent disease-2 and Lowe syndrome. *Nephrology, Dialysis, Transplantation: Official Publication of the European Dialysis and Transplant Association - European Renal Association* **37**:262-270 https://doi.org/10.1093/ndt/gfab274 | PubMed

**Shahin WS,** Ebed SO, Tyler SR, Miljkovic B, Choi SH, Zhang Y, Zhou W, Evans IA, Yeaman C, Engelhardt JF (2023) Redox-dependent Igfbp2 signaling controls Brca1 DNA damage response to govern neural stem cell fate. *Nature Communications* **14**:444 https://doi.org/10.1038/s41467-023-36174-z | PubMed

**Sharma S,** Skowronek A, Erdmann KS (2015) The role of the Lowe syndrome protein OCRL in the endocytic pathway. *Biological Chemistry* **396**:1293-1300 https://doi.org/10.1515/hsz-2015-0180 | PubMed

**Sharma Y,** Bhatia P, Rangappa G, Saha S, Raghu P (2025) Enhanced Notch dependent gliogenesis and delayed physiological maturation underlie neurodevelopmental defects in Lowe syndrome. *EMBO Molecular Medicine* **17**:3407-3439 https://doi.org/10.1038/s44321-025-00327-y | PubMed

**Wang W,** Esbensen Y, Kunke D, Suganthan R, Rachek L, Bjørås M, Eide L (2011) Mitochondrial DNA damage level determines neural stem cell differentiation fate. *The Journal of Neuroscience: The Official Journal of the Society for Neuroscience* **31**:9746-9751 https://doi.org/10.1523/JNEUROSCI.0852-11.2011 | PubMed

**Williams DM,** Gungordu L, Jackson-Crawford A, Lowe M (2022) Assessment of endocytic traffic and Ocrl function in the developing zebrafish neuroepithelium. *Journal of Cell Science* **135**:jcs260339 https://doi.org/10.1242/jcs.260339 | PubMed

**Zamanian JL,** Xu L, Foo LC, Nouri N, Zhou L, Giffard RG, Barres BA (2012) Genomic analysis of reactive astrogliosis. *The Journal of Neuroscience: The Official Journal of the Society for Neuroscience* **32**:6391-6410 https://doi.org/10.1523/JNEUROSCI.6221-11.2012 | PubMed

**Zhang Y,** Pak C, Han Y, Ahlenius H, Zhang Z, Chanda S, Marro S, Patzke C, Acuna C, Covy J, *et al.* (2013) Rapid single-step induction of functional neurons from human pluripotent stem cells. *Neuron* **78**:785-798 https://doi.org/10.1016/j.neuron.2013.05.029 | PubMed

**Zhuang T** (2025) Hedgehog pathway, cell cycle, and primary cilium. *Cell Death Discovery* **11**:302 https://doi.org/10.1038/s41420-025-02605-7 | PubMed

# Peer reviews

## Reviewer #2 (Public review):

Summary:

This manuscript investigates how neural cell development is affected in Lowe syndrome. Using neural cultures differentiated from human iPSCs carrying either a LS mutation or a genetically engineered mutation in OCRL, the authors show a depletion of mitochondrial DNA and decrease in mitochondrial activities that correlate with an increased formation of astrocytes at the expense of neurons. Similar effects on mitochondria and on astrocyte development were observed in a LS mouse model. Moreover, these mutant brain cells are less likely to be ciliated and show a reduction in Sonic hedgehog signalling.

Strengths/Weaknesses:

The study derives strength from the analyses of two different models of Lowe syndrome, both reaching similar conclusions. However, the observed changes in mitochondrial defects, neuronal/astrocytic development and primary cilia are only correlated, with no attempt to investigate a causal relationship. Moreover, the mouse model is only analysed at the adult stage providing no insights into the development of the defects. Different brain regions are analysed with immunostainings and qRT-PCR making it challenging to draw clear correlations between these findings. The quality of the corresponding figures is often poor and the selection of markers is frequently inappropriate. Taken together, these limitations complicate the interpretations of the data and significantly limit the conclusions that can be drawn from the study.

Although the study remains incomplete as main claims are only partially supported it can be used as a starting point for future functional studies into the link between mitochondrial defects and primary cilia in neural development.

Comments on revised version:

I am afraid the revised manuscript does little to address the concerns I raised in my initial review. The authors have primarily revised the text, removed over-interpretations and

discussed critical points as limitations of the study. This gives the impression that key concerns have merely been rationalised, particularly as only a few new experiments are presented. My main concerns therefore remain:

(1) The authors present three different phenotypes (altered neural differentiation, mitochondria dysfunction, alterations in primary cilia and ciliary Shh signalling) but a link between these phenotypes is not investigated. No mechanistic experiments are presented. Instead, the authors try to address the lack of a mechanism through refined wording but still use formulations that imply a direct link between these phenotypes. For example, their rebuttal letter finishes with the statement that the manuscript "provides a multi-model, cross-species framework linking mitochondrial dysfunction, ciliary signaling, and altered neural differentiation in Lowe syndrome". Similar formulations are used in the text.

(2) The authors still claim that ciliary Shh signalling is reduced but ignore the fact that Shh mRNA in iN cells and Shh protein in the IOB mouse are significantly decreased. This reduction represents the most likely explanation for the reduced levels of Gli1 and Ptc1 mRNAs (Shh target genes), rather than dysfunction of cilia. In order to test for cilia dysfunction, the authors need to use experiments in which they quantify the response of control and OCRL mutant cells to exogenously added Shh protein or Shh agonists. Moreover, the increased Gli1 protein expression in the IOB mouse contradicts the reduced levels of Gli1 mRNA.

(3) The analyses of the IOB mice are only done in 2 months old adult animals, nevertheless claims are made that changes in cell proportions are consequences of altered cell fate decisions. Alterations in proliferation and cell death are not addressed by experiments.

https://doi.org/10.7554/eLife.104055.2.sa1

## Author response:

The following is the authors' response to the original reviews.

> ***eLife Assessment***
>
> *This study investigated mitochondrial dysfunction and the impairment of the ciliary Sonic Hedgehog signaling in Lowe syndrome (LS), a timely topic given the limited research in this area. The data from patient iPSC-derived neurons and a mouse model were collected using solid methods, but the evidence supporting key claims is incomplete, and some technical aspects fall short of expectations. Despite these limitations, the study provides a useful foundation for exploring the relationship between mitochondrial defects and primary cilia in neural development.We appreciate the editorial assessment highlighting the importance of studying mitochondrial dysfunction and ciliary signaling in Lowe syndrome. We acknowledge that our study is largely associative, and we have revised the manuscript to clearly state this limitation, toned down causal claims, and emphasized that our work provides a foundation for future mechanistic studies.*

We appreciate the editorial assessment highlighting the importance of studying mitochondrial dysfunction and ciliary signaling in Lowe syndrome. We acknowledge that our study is largely associative, and we have revised the manuscript to clearly state this limitation, toned down causal claims, and emphasized that our work provides a foundation for future mechanistic studies.

We have also:

- Improved figure clarity and consistency

- Corrected errors in gene annotations and normalization

- Refined the mechanistic framework linking OCRL, mitochondria, and cilia

New Experimental Data:

Figure 5, Supplementary Figure 4. We confirmed mitochondrial defects by generating *ocrl*-KO zebrafish (Supplementary Figure 4). We first assessed mitochondrial reactive oxygen species (mitoROS) using MitoSOX staining. Next, we evaluated mitochondrial membrane potential (ΔΨm) using MitoTracker CMXRos. Finally, we assessed mitochondrial content via TOM20 staining. For all analyses, we focused on the ocular and cranial regions of the zebrafish to maintain consistency (see Author response image 1). Notably, previous studies have reported that *ocrl*-KO zebrafish exhibit seizures and brain developmental abnormalities, supporting their relevance as a model for Lowe syndrome-like phenotypes [1].

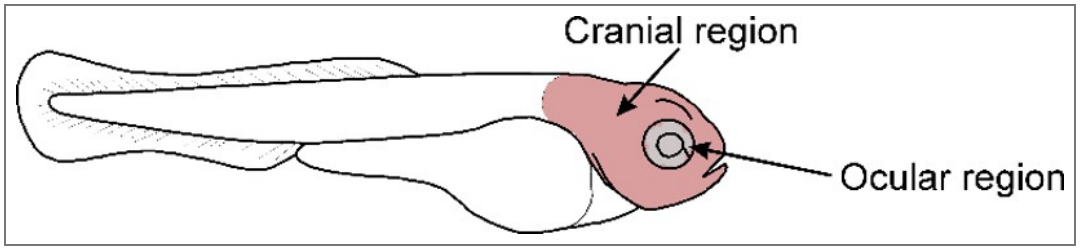


**Author response image 1.**

Figure 6 c. In addition to quantifying the proportion of ciliated cells in the IOB mouse brain, we measured cilia length and compared it between IOB and WT brain sections. Our results show that IOB mice exhibit elongated cilia compared to WT controls, suggesting that OCRL deficiency is associated with stress-related alterations in ciliary structure. These findings are consistent with previous studies reporting that cilia elongation can be associated with increased ROS levels and mitochondrial dysfunction [2,3].

> ***Public Reviews:***
>
> ***Reviewer #1 (Public review):***
>
> *The preparation of the manuscript requires improvement. There are many errors in the presentation of data.*

We thank the reviewer for this important comment. We have carefully revised the manuscript to improve the clarity, accuracy, and consistency of data presentation.

Specifically, we have corrected inconsistencies in gene nomenclature (e.g., CO2 vs COX2, DLOOP) across the text, figures, and legends. We standardized normalization methods and ensured consistency between figures and descriptions. We revised figure labels, legends, and annotations for clarity and accuracy. We corrected referencing errors and ensured appropriate citation of prior work. We improved overall figure quality and readability. In addition, we performed a thorough review of the entire manuscript to eliminate typographical errors and ensure consistency in terminology and data interpretation.

> *The use of references needs to be re-considered. Sometimes a reference is used when in fact the results included in that paper are the opposite of what the authors intend.*

We thank the reviewer for this important comment. We have carefully re-evaluated all references throughout the manuscript to ensure that they accurately reflect the findings they are cited to support. In cases where the cited studies did not fully align with our interpretation or could be misleading, we have either revised the text to more accurately

represent the original findings or replaced the references with more appropriate sources. We have also clarified instances where prior studies report differing or context-dependent results to avoid overinterpretation.

> *The authors conclude the paper by claiming that mitochondrial dysfunction and impairments of the ciliary SHH contribute to abnormal neuronal differentiation in LS, but the mechanism by which this sequence of events might happen hasn't been shown.*

We thank the reviewer for this important comment. We agree that the current study does not establish a direct causal mechanism linking mitochondrial dysfunction, ciliary SHH signaling, and altered neuronal differentiation in Lowe syndrome. Our data demonstrate that these processes co-occur consistently across multiple model systems, supporting a potential functional relationship. However, we acknowledge that the precise sequence of events and mechanistic connections remains to be defined. To address this, we have revised the manuscript to clarify that our conclusions are based on associative findings rather than direct mechanistic evidence. We have also updated the Discussion to explicitly acknowledge this limitation and to frame our model (Figure 7) as a proposed working hypothesis. Future studies will be required to determine whether mitochondrial dysfunction directly impacts ciliary SHH signaling and how these pathways influence neuronal differentiation.

> *Phenotype of increased astrocytes in both the IOB mouse brain or iPSC-derived cultures iN cells requires clarification as one of the markers used as an astrocyte marker, BRN2, is commonly used as a neuronal marker. As LS is a neurodevelopmental disorder, and the phenotype in question is related to differentiation, it is crucial to shed light on the developmental timeline in which this phenotype is seen in the mouse brain.*

We thank the reviewer for this important comment. We agree that the use of BRN2 as an astrocytic marker was inappropriate, as it is primarily recognized as a neuronal marker. Accordingly, we have revised the manuscript to remove BRN2 from the interpretation of astrocytic identity and now rely on GFAP expression as the primary astrocytic marker. We have also clarified this point in both the Results and figure legends to avoid misinterpretation. In addition, we have revised the text to more accurately describe our findings as an altered balance in neuronal versus astrocytic marker expression, rather than a definitive increase in astrocyte numbers.

Regarding the developmental context, we acknowledge that Lowe syndrome is a neurodevelopmental disorder and that temporal aspects are highly relevant. In our study, the *in vivo* analyses were performed on adult 2-month-old IOB mouse brains, which we have now explicitly stated in the manuscript. We recognize that this limits our ability to directly assess developmental dynamics of lineage specification. We have therefore added this as a limitation in the Discussion and clarified that future studies examining earlier developmental stages will be necessary to determine when these alterations arise.

> *Mitochondrial dysfunction in astrocytes has been shown to induce a ciliogenic program. However, almost the opposite is shown in this paper, with regards to ciliation. Morphology of the cilia was not assessed either, which is an important feature of ciliary homeostasis. The improper ciliary homeostasis here appears to be the improper Shh signalling, which has not been shown to be related to mitochondrial dysfunction. This leaves one wondering how exactly the different phenotypes shown in this paper are connected.*

We thank the reviewer for this important comment. We agree that the relationship between mitochondrial dysfunction, ciliogenesis, and Shh signaling is complex and not fully resolved in the current study.

As noted by the reviewer, prior studies have reported that mitochondrial dysfunction can

promote a ciliogenic program [4]. In contrast, our data show a reduced proportion of ciliated cells together with increased cilia length, indicating altered ciliary homeostasis rather than a straightforward increase in ciliogenesis. To address this point, we have revised the manuscript to describe our findings as context-dependent alterations in ciliary parameters more clearly, and we now explicitly discuss this apparent discrepancy with the literature in the Discussion. We also acknowledge the reviewer's point regarding ciliary morphology. In the revised manuscript, we have included quantification of cilia length in addition to the proportion of ciliated cells, and we have expanded the Methods section to detail how these measurements were performed. We agree that additional ultrastructural and functional analyses would further strengthen the characterization of ciliary homeostasis, and we now include this as a limitation and future direction.

Regarding the link between mitochondrial dysfunction, ciliary alterations, and Shh signaling, we agree that our study does not establish a direct mechanistic connection. Our data demonstrate that these phenotypes co-occur consistently across multiple models, but do not define causality. To address this concern, we have revised the manuscript to clarify that our conclusions are associative, and we now present our integrated model (Figure 7) as a working hypothesis rather than a demonstrated mechanism. We also explicitly state in the Discussion that future studies will be required to determine whether mitochondrial dysfunction directly impacts ciliary signaling and Shh pathway activity.

> *This paper lacks a clear mechanistic approach. While the data validates the 3 broad phenotypes mentioned, there is a lack of connection between these phenotypes or an answer to why these phenotypes appear. While the discussion attempts to shed light on this by referencing previous studies, some of the referenced studies show contradicting results. Hence, it would be beneficial to clarify these gaps with further experiments and address the larger question of the connection between the mitochondria, Shh signalling, and astrocyte formation.*

We thank the reviewer for this important and insightful comment. We agree that the current study does not establish a direct mechanistic link connecting mitochondrial dysfunction, altered Shh signaling, and changes in neuronal versus astrocytic differentiation.

Our primary goal in this work was to identify and validate phenotypes associated with OCRL deficiency across multiple independent model systems. We demonstrate that mitochondrial dysfunction, oxidative stress, altered ciliary/Shh signaling, and changes in neural lineage-associated markers co-occur consistently in these models. However, we acknowledge that the causal relationships between these processes remain to be defined.

To address this concern, we have revised the manuscript to more clearly state that our conclusions are associative rather than mechanistic, and we now present our integrated model (Figure 7) as a working hypothesis that links these phenotypes through a potential mitochondria-ROS-signaling axis. We have also expanded the Discussion to explicitly acknowledge this limitation and to avoid overinterpretation of causality.

In addition, we have carefully re-evaluated and revised the cited literature to ensure accuracy, particularly in cases where prior studies report context-dependent or seemingly contradictory effects of mitochondrial dysfunction on ciliogenesis and signaling pathways. These points are now discussed more explicitly to better position our findings within the existing literature.

We agree that further experiments, such as targeted rescue of mitochondrial function or modulation of Shh signaling, will be necessary to establish causal relationships between these pathways. These directions are now clearly outlined in the revised Discussion as important next steps.

> *Most importantly, there is no mention of how the loss of OCRL, a 5-phosphatase enzyme, results in the appearance of the mentioned phenotypes. Since there are multiple studies in the field of Lowe Syndrome that shed light on the various functions of OCRL, both catalytic and non-catalytic, it is important to address the role of OCRL in resulting in these phenotypes.*

We thank the reviewer for this important comment. We agree that the link between OCRL function and the observed phenotypes was not sufficiently developed in the original version of the manuscript.

In the revised manuscript, we have expanded the Discussion to more clearly outline how loss of OCRL could contribute to the observed mitochondrial, ciliary, and differentiation phenotypes. OCRL encodes a PI(4,5)$P_2$ 5-phosphatase that regulates phosphoinositide homeostasis and membrane dynamics. Disruption of this activity is known to affect endolysosomal trafficking, actin organization, and membrane remodeling-processes that are critical for organelle maintenance and ciliary function. We now discuss how these alterations could impact mitochondrial homeostasis, for example, through defects in membrane contact sites, vesicular trafficking, or organelle quality control pathways.

In addition, we have incorporated discussion of potential non-catalytic roles of OCRL, including protein–protein interactions and scaffolding functions, which may contribute to the coordination of intracellular trafficking and cytoskeletal organization. These aspects may provide an additional layer of regulation linking OCRL loss to both mitochondrial dysfunction and ciliary alterations.

We emphasize that, while these mechanisms are supported by prior studies, our data do not directly test them. Therefore, we have carefully framed this section as a plausible mechanistic framework rather than a demonstrated pathway and have explicitly stated this limitation. We also outline future experiments aimed at dissecting catalytic versus non-catalytic contributions of OCRL to these phenotypes.

> *There are numerous errors in the qPCR experiments performed concerning the genes that were assayed. The genes mentioned in the text section do not match those indicated in the graphs or legends. This takes away the confidence of the reader in this data.*

We thank the reviewer for this important observation. We agree that the inconsistencies between the genes described in the text and those shown in the figures and legends could reduce confidence in the data. In the revised manuscript, we have carefully rechecked all qPCR experiments and corrected the gene names across the Results, figures, and figure legends to ensure full consistency. We have also standardized the nomenclature throughout the manuscript (including consistent use of gene symbols and formatting) and verified that all plotted data correspond to the correct targets.

In addition, we have clarified the qPCR methodology, including normalization (all data are normalized to GAPDH) and primer information, to improve transparency and reproducibility.

> ***Reviewer #2 (Public review):***
>
> *Summary:*
>
> *This manuscript investigates how neural cell development is affected in Lowe syndrome. Using neural cultures differentiated from human iPSCs carrying either an LS mutation or a genetically engineered mutation in OCRL, the authors show a depletion of mitochondrial DNA and a decrease in mitochondrial activities that correlate with an increased formation of astrocytes at the expense of neurons. Similar effects on mitochondria and on astrocyte development were observed in an LS mouse model.*

> *Moreover, these mutant brain cells are less likely to be ciliated and show a reduction in Sonic Hedgehog signalling.*
>
> *Strengths/Weaknesses:*
>
> *The study derives strength from the analyses of two different models of Lowe syndrome, both reaching similar conclusions. However, the observed changes in mitochondrial defects, neuronal/astrocytic development, and primary cilia are only correlated, with no attempt to investigate a causal relationship. Moreover, the mouse model is only analysed at the adult stage providing no insights into the development of the defects. Different brain regions are analysed with immunostainings and qRT-PCR making it challenging to draw clear correlations between these findings. The quality of the corresponding figures is often poor and the selection of markers is frequently inappropriate. Taken together, these limitations complicate the interpretations of the data and significantly limit the conclusions that can be drawn from the study.*

We have carefully revised the manuscript to address the concerns raised, and we have revised the manuscript with additional supporting data.

> ***Recommendations for the authors:***
>
> ***Reviewer #1 (Recommendations for the authors):***
>
> *The authors have checked the expression of neuronal markers NeuN and FoxG1, and apart from GFAP, they categorise Brn2 as one of the astrocytes markers that they have also checked. But Brn2 is not an astrocyte marker. It is a neuronal marker that is expressed in layer 2/3 of the cortex. In fact, Brn2 is reported to be a key driver of neurogenesis in primate telencephalon development1 and for reprogramming of astrocytes to neurons2. Hence, the only glial marker they have used here is GFAP. BRN2 is a neuronal marker. It has been used as a neuronal marker even in the reference (Zhang et al, 2013), from which the protocol for inducing iPSCs to induced neurons (iNs) was taken. Hence, the qPCR results in 1g of overexpression of BRN2 indicate an increase in expression of a neuronal marker, not an astrocyte marker.*

We thank the reviewer for this important and well-founded comment. We fully agree that BRN2 is a neuronal marker and not an astrocytic marker, and that its inclusion as an astrocyte marker in our original interpretation was incorrect.

In the revised manuscript, we have removed BRN2 from the analysis and interpretation of astrocytic identity. We now treat BRN2 exclusively as a neuronal marker and have updated the Results, figure legends, and text accordingly. Specifically, the qPCR data previously presented in Figure 1g are now interpreted as reflecting neuronal marker expression, not astrocytic differentiation. We have also revised our conclusions to avoid overinterpretation of astrocyte abundance. Our findings are now described more accurately as an altered balance in neuronal versus astrocytic marker expression, rather than a definitive increase in astrocyte numbers. In this context, GFAP remains the primary astrocytic marker used in this study.

We acknowledge the reviewer's point that reliance on a single astrocytic marker is a limitation. This has now been explicitly stated in the Discussion, and we note that additional astrocyte markers will be required in future studies to more comprehensively define lineage-specific changes.

> *Incorrect marker usage (BRN2 as astrocyte marker)*

We thank the reviewer for identifying this critical issue. We corrected the classification of BRN2 as a neuronal marker. Also, we re-analyzed the interpretation accordingly, revised all

relevant text and figures. Importantly, Astrocyte conclusions are now based primarily on GFAP expression, and we explicitly acknowledge this limitation in the Discussion

> *The graphs for the RT-PCR results indicate that gene expression values are normalized to actin whereas the legend mentions that they are normalized to GAPDH. This needs clarification.*

We thank the reviewer for pointing out this inconsistency. We confirm that all qPCR data were normalized to GAPDH, and the reference to actin was an error. This has now been corrected throughout the figures, legends, and text to ensure consistency.

> *The use of wording to refer to the generation of induced neurons (iNs) should ideally be changed from "we developed"; as the protocol from Zhang et al, 2013 seems to have been directly adapted in this paper.*

We thank the reviewer for this helpful suggestion. We agree that the wording was inappropriate. In the revised manuscript, we have replaced “we developed” with language indicating that iNs were generated using an established protocol, and we now explicitly state that the method was adapted from Zhang et al., 2013 [5].

> *OCRL KO iPSCs were obtained from Herbert Lachman's lab and not generated in this study. Hence, the Ran et al, 2013 reference is not necessary.*

We thank the reviewer for this clarification. We agree that the OCRL knockout iPSCs were obtained from Herbert Lachman’s laboratory and were not generated in this study. Accordingly, we have removed the Ran et al., 2013 reference and revised the manuscript to clearly state the origin of the OCRL KO iPSC line.

> *The reference for Figure 1c is given as Ran et al, 2013 which is wrong. It should be Zhang et al, 2013.*

We thank the reviewer for noting this error. We have corrected the reference for Figure 1c from Ran et al., 2013 to Zhang et al., 2013 in the revised manuscript.Limited *in vivo* mitochondrial characterization

> *Figure 1D, E: GFAP is a cytoskeletal marker but its expression here is very grainy and looks like an artifact. Is it possible to show the astrocyte phenotype using other astrocytes nuclei and cytosolic markers such as NFIA and S100B, respectively?*

We thank the reviewer for this important suggestion. We acknowledge that GFAP is a cytoskeletal marker and that the signal in the current images may appear granular. We have carefully re-evaluated the staining and image processing to ensure that the signal represents true GFAP expression and have improved the image quality and presentation in the revised figures. We agree that inclusion of additional astrocytic markers such as NFIA and S100B would further strengthen the characterization. While we were not able to include these additional markers in the current revision, we now explicitly acknowledge this as a limitation in the Discussion and note that future studies will incorporate a broader panel of astrocyte markers to more comprehensively define astrocytic identity.

> *Since the authors have not used enough markers to understand the cell-type composition in WT and OCRL KO/mutant lines, it's not sufficient to conclude that the NPCs preferentially favour astrocytes over neuronal lineage. Any conclusive comments regarding the cell-state/cell-type specification necessitate evidence such as genetic lineage tracing using reporters for neuronal and astrocyte markers, and/or RNA/ATAC/scRNA sequencing.*

We thank the reviewer for this important point. We agree that the current marker panel is not sufficient to definitively determine cell-type composition or to conclude preferential

lineage specification.

In the revised manuscript, we have tempered our conclusions and now describe our findings as changes in neuronal versus astrocytic marker expression, rather than evidence of a shift in lineage fate. We also explicitly acknowledge this limitation in the Discussion. We agree that approaches such as genetic lineage tracing, reporter-based assays, and single-cell transcriptomic or epigenomic analyses (e.g., scRNA-seq or scATAC-seq) would be required to rigorously define cell-state transitions and lineage outcomes. These are important directions for future studies and are now highlighted in the revised manuscript.

> *Figure 2:*
>
> *The mt-DNA gene CO2 was checked, not COX2. A typographical error in the written section, which does not match with the qPCR graph of the same.*

We thank the reviewer for noting this inconsistency. We confirm that the gene analyzed was CO2, and the reference to COX2 in the text was incorrect. This has now been corrected throughout the manuscript to ensure consistency between the text, figures, and qPCR data.

> *The word "neurogenesis" is used very loosely throughout the paper. In the opinion of the reviewer, there is no evidence presented that there is a defect in neurogenesis in either of the models used in this paper.*

We thank the reviewer for this important comment. We agree that the term “neurogenesis” was used too broadly and is not directly supported by our data. In the revised manuscript, we have removed or replaced this term where appropriate and now refer more precisely to changes in neuronal versus astrocytic marker expression.

> *Line 150: They say that they have examined the functional properties of mitochondria during neurogenesis but it would have been better to understand OXPHOS at various time points of neurogenesis to actually conclude reduced OXPHOS 'during neurogenesis'. Moreover, genes related to other pathways such as glycolysis could have been checked to understand the bioenergetics of LS patients. Also, oxidative stress could have been checked using more than one marker. Since they are trying to understand the functional role of mitochondrial defects during neurogenesis, they could have performed live imaging of mitochondrial potential during various stages of neurogenesis. Isolation of mitochondria from LS patients and transcriptomics/proteomics might provide further clues about mitochondrial defects.*

We thank the reviewer for these thoughtful suggestions. We agree that our data do not capture mitochondrial function across multiple stages of neurogenesis. In the revised manuscript, we have modified the wording to avoid implying temporal analysis “during neurogenesis” and instead describe mitochondrial parameters in differentiated cells. To strengthen the study, we have included additional *in vivo* validation in the zebrafish model, where we assessed multiple mitochondrial readouts, including mitochondrial membrane potential (ΔΨm) using MitoTracker CMXRos, oxidative mitochondrial stress ROS (mitoROS) using MitoSOX staining, and mitochondrial content (TOM20), supporting mitochondrial dysfunction across systems.

> *Elevated astrocytic reaction during the differentiation of NSPCs in the Lowe syndrome (IOB) mouse model.*
>
> *Title: What does astrocyte reaction mean? This term should not be used without clear evidence of reactive astrocytes being present in the model.*

We thank the reviewer for this important comment. We agree that the term “astrocytic reaction” is not appropriate without specific evidence of reactive astrocytes. In the revised

manuscript, we have removed this terminology and replaced it with more accurate wording, describing our findings as altered astrocytic marker expression. This change better reflects the data and avoids overinterpretation.

> *In 1a, no quantification of the mouse brain size is given. From the given images alone, there appears to be no obvious decrease in brain size between the WT and IOB mice. This contradicts the text which indicates that the IOB mouse brain is smaller.*

We appreciate this important point. We have:

Removed claims regarding reduced brain size

Clarified that our analysis was limited to available sections and no definitive conclusion about global brain morphology can be made

> *Figure 3E: Why is the astrocyte to neuron ratio measured using a cytoskeletal marker for astrocytes, GFAP but a nuclear marker for neurons, NeuN? Ratios to measure the percentage or proportion of astrocytes to neurons can only be checked by markers of the same nature such as GFAP to MAP2 (neuronal cytoskeletal marker) or NFIA (astrocyte nuclear marker) to NeuN.*

We thank the reviewer for this important point. We agree that comparing a cytoskeletal marker (GFAP) with a nuclear marker (NeuN) is not ideal for deriving cell-type ratios. In the revised manuscript, we have removed the astrocyte-to-neuron ratio analysis and now present these data as relative marker expression/signals rather than proportions. We have also clarified this limitation in the text and Discussion.

> *(3) Lack of clarity in the experiments performed on the mice brains. PAX6 is used here as a neuronal marker along with NeuN, a mature neuronal marker. This is misleading as PAX6 is rather a marker for neural stem/progenitor cells and not neurons. The age of the mice has also not been mentioned, which is crucial considering the different markers used to characterize the mouse brain as well as since the authors are indicating that there is an abnormal neurodevelopment in the IOB mouse during development. Again, BRN2 is used here as an astrocyte marker. However, it is a neuronal marker. Hence, the phenotype of increased astrocytes currently is held by GFAP expression alone. Another astrocyte marker should be used.*

We thank the reviewer for these important points. We have revised the manuscript to correct marker interpretation, now describing PAX6 as a progenitor marker rather than neuronal, and BRN2 as a neuronal marker, removing it from astrocyte-related analysis. We have also explicitly stated the age of the mice (2 months) in the Methods and Results. In addition, we have tempered our conclusions, describing the data as changes in marker expression rather than definitive cell-type shifts, and we now acknowledge that reliance on GFAP as a single astrocytic marker is a limitation, which is discussed in the revised manuscript.

> *Figure 6: Increase in astrocytes, mitochondrial dysfunction, and ciliary Shh signalling are 3 phenotypes discussed in this study. However, no experiments were done to shed light on the mechanistic connection between these phenotypes. This is reflected in the abstract shown in Figure 6. There is no comment on the mechanism behind these phenotypes.*

We thank the reviewer for this important comment. We agree that the current study does not establish a direct mechanistic link between mitochondrial dysfunction, altered ciliary Shh signaling, and changes in astrocytic markers. Our aim was to identify and validate these phenotypes across multiple models. In the revised manuscript, we have clarified that Figure 7 represents a proposed working model based on associative findings rather than a defined mechanism. We have also revised the Discussion to explicitly acknowledge this limitation and to outline future experiments required to establish causal relationships between these

> ***Reviewer #2 (Recommendations for the authors):***
>
> *The authors report interesting findings in two different experimental models but the manuscript would benefit significantly from an analysis of a potential causal relationship between different findings. They often mention neural stem cells or the neuron/glia switch but their analysis of the mouse mutant is restricted to the adult stage. A more consistent analysis of specific brain regions would also be beneficial.*

We thank the reviewer for this constructive comment. We agree that establishing causal relationships between the observed phenotypes is an important next step. In the revised manuscript, we have clarified that our conclusions are based on associative findings and have expanded the Discussion to outline experimental strategies that could address causality in future studies. We also acknowledge that our *in vivo* analysis is restricted to adult (2-month-old) IOB mouse brains, which limits our ability to assess developmental dynamics such as neural stem cell behavior or neuron-glial transitions. This limitation is now explicitly stated in the Discussion. Finally, we agree that region-specific analysis would strengthen the study. Due to the availability of samples, our analysis was not systematically performed across defined brain regions. We now acknowledge this limitation and note that future studies focusing on specific regions (e.g., cortex, hippocampus) will be important to better understand the spatial aspects of the phenotype.

> *Figure 1: The authors only measured the expression of marker genes by qRT-PCR. This could reflect higher expression levels in individual cells rather than a change in the proportion of neurons and astrocytes. They need to determine the cell proportions of astrocytes and neurons in addition. Moreover, there is a poor marker choice. Loss of FOXG1 expression could indicate a loss of telencephalic identity. BRN2 is expressed by cortical neurons.*

We thank the reviewer for this important comment. We agree that qPCR-based marker analysis does not directly reflect cell-type proportions and may instead represent changes in gene expression per cell. Accordingly, we have revised the manuscript to avoid conclusions about cell proportions and now describe the data as changes in marker expression. We have also corrected marker interpretation, removing BRN2 from astrocyte analysis and clarifying that FOXG1 reflects telencephalic identity. These limitations and the need for more comprehensive cell-type characterization are now acknowledged in the Discussion.

> *In Figure 2, the authors determine the properties of mitochondria and claim that functional mitochondrial activities are decreased during neurogenesis in mutant iN cells. They need to take into account that according to Figure 1 the proportion of neurons and astrocytes may be changed. Hence, the decreased mitochondrial activity may reflect a fundamental difference between neurons and astrocytes. The authors need to clearly distinguish between neurons and astrocytes in their analysis. Moreover, the use of the term neurogenesis is confusing. They are analysing the neuron-to-glial switch, not the formation of neurons.*

We thank the reviewer for this important comment. We agree that differences in cell-type composition may influence mitochondrial measurements. In the revised manuscript, we have tempered our interpretation, describing these data as changes in mitochondrial parameters at the population level rather than neuron-specific effects. We also acknowledge this limitation in the Discussion and note that cell-type-specific analyses will be required in future studies. In addition, we have revised the terminology throughout the manuscript, removing the term “neurogenesis” and instead referring to changes in neuronal versus glial marker expression to more accurately reflect the scope of our analysis.

> *Figure 3: The authors claim that astrocyte numbers are elevated in the IOB mouse model,*

> *however, it seems as if the authors analysed late postnatal, potentially adult brains but no age of the brains is provided. Given the large time lag between the formation of astrocytes and their analysis, the increased number of astrocytes could be due to a number of processes including altered proliferation and cell death. The authors need to investigate the proportion of astrocytes and neurons closer to the neuron-to-glia switch. Cell fate experiments like the long-term application of BrdU would be much better suited and would provide mechanistic insights. Again, markers are not adequate to reach their conclusion. Pax6 is only expressed in a tiny subset of neurons, Brn2 on the other hand is not astrocyte-specific as it is expressed in cortical neurons as well. Moreover, qRT-PCR analyses were done in the cortex and hippocampus whereas the boxes in Figure 3D are located in the basal ganglia. It would be much more informative and provide better comparisons to perform gene expression analysis and cell counts in the same brain regions.*

We thank the reviewer for these important and constructive comments. We agree that our analysis is limited by the use of adult (2-month-old) IOB mouse brains, which do not allow direct assessment of developmental processes such as the neuron-to-glia transition. We have now explicitly stated the age of the animals and clarified this limitation in the Discussion, including the possibility that changes in astrocytic markers may reflect processes such as proliferation or survival rather than lineage specification.

We also agree that our marker panel was insufficient for definitive conclusions. Accordingly, we have revised the manuscript to remove overinterpretation, corrected marker usage, and now describe the data as changes in marker expression rather than cell-type proportions. The need for more rigorous approaches, such as lineage tracing (e.g., BrdU) and expanded marker panels, is now acknowledged as a future direction. Finally, we thank the reviewer for pointing out the inconsistency in the brain regions analyzed. We have clarified the regions used for qPCR, and we now explicitly acknowledge this limitation, noting that future studies will aim to perform region-matched molecular and histological analyses for more accurate comparisons.

> *Experiments in Figure 4 assess "whether changes in mitochondrial activity are involved in the altered differentiation of stem cells and progenitor cells in the LS mouse model" in 3-month-old brain sections. The murine adult brain only contains a few neural stem cells in the SVZ and in the dentate gyrus. Instead, this analysis needed to be done at late embryonic/early postnatal stages to capture the neuronal/glial switch. In addition, RT-PCR and immunostainings should be performed in the same brain region as stated above.*

We thank the reviewer for this important point. We agree that analysis in adult (2-month-old) brains does not capture developmental stages such as the neuron-glia transition. We have revised the manuscript to remove implications of developmental analysis and now describe these data as mitochondrial parameters in adult tissue, explicitly acknowledging this limitation in the Discussion. We also clarify the brain regions used for qPCR and immunostaining and note as a limitation that these were not fully matched; future studies will perform region-specific, developmentally timed analyses.

> *Figure 5: The authors examine a potential link between mitochondrial defects and primary cilia. Mutant iN cell cultures contain lower levels of SHH mRNA and show concomitantly lower expression of the SHH target genes GLI1 and PTCH1. The authors link this finding with a reduced proportion of ciliated cells but the reduced SHH signalling is most likely explained by the decreased SHH expression. The authors also limit their analysis of primary cilia to one brain region, but they should also include the cortex and hippocampus as these regions were used for their qRT-PCR analysis. SHH signalling acts as a switch to stop the proteolytic processing of GLI3 and to promote the formation of the GLI3 activator form. It is therefore important to determine the ratio of GLI3 repressor*

> *and GLI3 activator using western blots. The authors claim that they found defective cilia formation, but cilia are poorly characterised. Are there differences in intraflagellar transport, the formation of the transition zone, etc? Is ciliary length altered? The authors only make a correlative link between mitochondrial defects and cilia but present no experiments to investigate causation. They should at least discuss potential mechanisms which could explain defects in cilia.*

We thank the reviewer for these insightful comments. We agree that reduced SHH pathway activity may be influenced by decreased SHH expression, and we have revised the text to avoid overattributing this effect to ciliary changes. Our conclusions are now framed as associative, not causal.

We have expanded our cilia analysis to include quantification of both the proportion of ciliated cells and cilia length, and clarified these methods in the manuscript. We also acknowledge that additional characterization (e.g., intraflagellar transport, transition zone structure, GLI3 activator/repressor ratios) would further strengthen the analysis, and we now include this as a limitation and future direction. Regarding regional analysis, we agree that broader brain region coverage would be valuable. Due to sample availability, our analysis was limited, and this is now explicitly acknowledged as a limitation, with future studies aimed at region-matched analyses (e.g., cortex and hippocampus). Finally, we have expanded the Discussion to outline potential mechanisms linking mitochondrial dysfunction and ciliary alterations, while clearly stating that causal relationships remain to be established.

> *(1) The methods section does not contain any information on how immunostainings on brain sections were performed.*

We agree that the description of immunostaining on brain sections was missing. We have now added a detailed protocol for brain section immunostaining in the Methods section to improve clarity and reproducibility.

> *(2) The abbreviation "RT-PCR" is used for both, real-time PCR and reverse transcription PCR*

We also acknowledge the inconsistent use of the term “RT-PCR.” In the revised manuscript, we have standardized the terminology, using “qPCR” (quantitative real-time PCR) throughout to avoid confusion

Conclusion

We believe that these revisions significantly strengthen the manuscript. While the study remains primarily associative, it provides a multi-model, cross-species framework linking mitochondrial dysfunction, ciliary signaling, and altered neural differentiation in Lowe syndrome.

References:

(1) Ramirez IB-R, Pietka G, Jones DR, Divecha N, Alia A, Baraban SC, et al. Impaired neural development in a zebrafish model for Lowe syndrome. Hum Mol Genet. 2012;21:1744–59. *https://doi.org/10.1093/hmg/ddr608*

(2) Kim JI, Kim J, Jang H-S, Noh MR, Lipschutz JH, Park KM. Reduction of oxidative stress during recovery accelerates normalization of primary cilia length that is altered after ischemic injury in murine kidneys. Am J Physiol Renal Physiol. 2013;304:F1283-1294. *https://doi.org/10.1152/ajprenal.00427.2012*

(3) Moruzzi N, Valladolid-Acebes I, Kannabiran SA, Bulgaro S, Burtscher I, Leibiger B, et al. Mitochondrial impairment and intracellular reactive oxygen species alter primary cilia morphology. Life Sci Alliance. 2022;5:e202201505. *https://doi.org/10.26508/lsa.202201505*

(4) Ignatenko O, Malinen S, Rybas S, Vihinen H, Nikkanen J, Kononov A, et al. Mitochondrial dysfunction compromises ciliary homeostasis in astrocytes. J Cell Biol. 2022;222:e202203019. *https://doi.org/10.1083/jcb.202203019*

(5) Zhang Y, Pak C, Han Y, Ahlenius H, Zhang Z, Chanda S, et al. Rapid Single-Step Induction of Functional Neurons from Human Pluripotent Stem Cells. Neuron. 2013;78:785–98. *https://doi.org/10.1016/j.neuron.2013.05.029*

https://doi.org/10.7554/eLife.104055.2.sa0